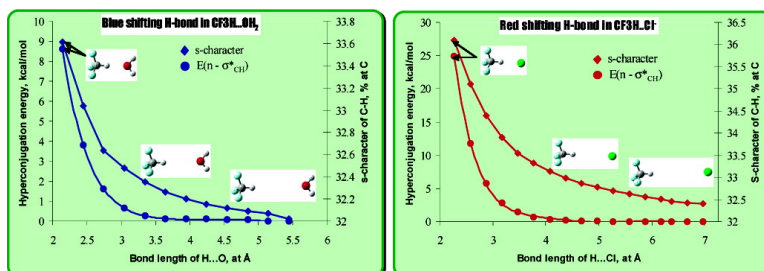


Electronic Basis of Improper Hydrogen Bonding: A Subtle Balance of Hyperconjugation and Rehybridization

Igor V. Alabugin, Mariappan Manoharan, Scott Peabody, and Frank Weinhold

J. Am. Chem. Soc., **2003**, 125 (19), 5973-5987 • DOI: 10.1021/ja034656e • Publication Date (Web): 19 April 2003

Downloaded from <http://pubs.acs.org> on March 26, 2009



More About This Article

Additional resources and features associated with this article are available within the HTML version:

- Supporting Information
- Links to the 48 articles that cite this article, as of the time of this article download
- Access to high resolution figures
- Links to articles and content related to this article
- Copyright permission to reproduce figures and/or text from this article

[View the Full Text HTML](#)

Electronic Basis of Improper Hydrogen Bonding: A Subtle Balance of Hyperconjugation and Rehybridization

Igor V. Alabugin,^{*,†} Mariappan Manoharan,[†] Scott Peabody,[†] and Frank Weinhold[‡]

Contribution from the Department of Chemistry and Biochemistry, Florida State University, Tallahassee, Florida 32306-4390, and Theoretical Chemistry Institute and Department of Chemistry, University of Wisconsin–Madison, Madison, Wisconsin 53706

Received February 13, 2003; E-mail: alabugin@chem.fsu.edu.

Abstract: The X–H bond length in X–H...Y hydrogen bonded complexes is controlled by a balance of two main factors acting in opposite directions. “X–H bond lengthening” due to $n(Y) \rightarrow \sigma^*(H-X)$ hyperconjugative interaction is balanced by “X–H bond shortening” due to increase in the s-character and polarization of the X–H bond. When hyperconjugation dominates, X–H bond elongation is reflected in a concomitant red shift of the corresponding IR stretching frequency. When the hyperconjugative interaction is weak and the X-hybrid orbital in the X–H bond is able to undergo a sufficient change in hybridization and polarization, rehybridization dominates leading to a shortening of the X–H bond and a blue shift in the X–H stretching frequency.

Introduction

Hydrogen bonding is essential to many chemical and biochemical processes.¹ A characteristic feature of H...Y hydrogen bond formation in an X–H...Y system is X–H bond lengthening with a concomitant red shift of the X–H stretching frequency. The latter, readily observed in the IR spectra, is widely regarded as the “signature of H-bonding”.² However, a number of experimental^{3,4,5} and theoretical⁶ studies have reported the existence of an unusual class of “improper” or “blue-shifted” hydrogen bonds in which H-bond formation leads to X–H bond shortening and to a blue shift of the X–H IR stretching frequency.⁷ Although this effect has been reported mainly for C–H bonds, recent theoretical studies suggest that improper H-bonding is more general and can be observed for Si–H,⁸ P–H,⁸ and even N–H^{8,9} bonds.

From its very discovery, improper hydrogen bonding received much attention from theoreticians who suggested several explanations for this phenomenon. Because several detailed discussions are available,^{7,8,10} we limit ourselves to a brief

outline of the most fundamental differences between the alternative explanations. The first line of thought, introduced by Hobza and co-workers,⁷ concentrated on differences between classical and improper H-bonding such as an increased importance of disperse interactions and of changes in the remote parts of the molecule, e.g., electron transfer to C–F bonds in a complex of fluoroform and water which occur in addition to more common hyperconjugative charge transfer from the lone pair of a heteroatom¹¹ to the σ^* (C–H) orbital ($n \rightarrow \sigma^*(C-H)$ interaction).²⁸ The second school of thought views conventional

[†] Department of Chemistry and Biochemistry, Florida State University.

[‡] Theoretical Chemistry Institute and Department of Chemistry, University of Wisconsin–Madison.

- (1) Scheiner, S. *Hydrogen Bonding*; Oxford University Press: New York, 1997.
- (2) Jeffrey, G. A. *An Introduction to Hydrogen Bonding*; Oxford University Press: New York, 1997.
- (3) Desiraju, G. R.; Steiner, T. *The Weak Hydrogen Bond*; Oxford University Press: Oxford, 1999.
- (4) Allerhand, A.; Schleyer, P. v. R. *J. Am. Chem. Soc.* **1963**, *85*, 1715.
- (5) Buděšinsky, M.; Fiedler, P.; Arnold, Z. *Synthesis* **1989**, 858.
- (6) Boldeskul, I. E.; Tsymbal, I. F.; Ryltsev, E. V.; Latajka, Z.; Barnes, A. J. *J. Mol. Struct.* **1997**, *436*, 167.
- (7) Hobza, P.; Spirko, V.; Havlas, Z.; Buchhold, K.; Reimann, B.; Barth, H.-D.; Brutschy, B. *Chem. Phys. Lett.* **1999**, *299*, 180.
- (8) Reimann, B.; Buchhold, K.; Vaupel, S.; Brutschy, B.; Havlas, Z.; Hobza, P. *J. Phys. Chem. A* **2001**, *105*, 5560.
- (9) Delanoye, S. N.; Herrebout, W. A.; van der Veken, B. J. *J. Am. Chem. Soc.* **2002**, *124*, 11 854–11 855.
- (10) Hobza, P.; Spirko, V.; Selzle, H. L.; Schlag, E. W. *J. Phys. Chem. A* **1998**, *102*, 2501.
- (11) Hobza, P.; Havlas, Z. *Chem. Phys. Lett.* **1999**, *303*, 447.

- (7) Hobza, P.; Havlas, Z. *Chem. Rev.* **2000**, *100*, 4253.
- (8) Li, X.; Liu, L.; Schlegel, H. B. *J. Am. Chem. Soc.* **2002**, *124*, 9639.
- (9) Fang, Y.; Fan, J.-M.; Liu, L.; Li, X.-S.; Guo, Q.-X. *Chem. Lett.* **2002**, 116.
- (10) Fan, J. M.; Liu, L.; Guo, Q.-X. *Chem. Phys. Lett.* **2002**, *365*, 464.
- (11) Hermansson, K. *J. Phys. Chem. A* **2002**, *106*, 4695.
- (12) In the literature discussion of hydrogen bonding, terms “donor” and “acceptor” are used in two different contexts. “H-bond donor” is the X–H part of the X–H...Y complex where Y is called “H-bond acceptor”. However, if the hyperconjugative flow of electrons in Lewis type electron donor/electron acceptor interaction is described, then $\sigma^*(X-H)$ is a Lewis (hyperconjugative) acceptor and lone pair of Y is a Lewis (hyperconjugative) donor. “H-bonds acceptors” are, in fact, electron donors in charge-transfer hyperconjugative (CT) $n(Y) \rightarrow \sigma^*(X-H)$ interactions.
- (13) (a) Scheiner, S.; Grabowski, S. J.; Kar, T. *J. Phys. Chem. A* **2001**, *105*, 10 607. (b) Scheiner, S.; Kar, T. *J. Phys. Chem. A* **2002**, *106*, 1784.
- (14) Gu, Y.; Kar, T.; Scheiner, S. *J. Am. Chem. Soc.* **1999**, *121*, 9411.
- (15) Bader, R. W. F. *Atoms in Molecules. A Quantum Theory*; Oxford University Press: Oxford, U.K., 1990.
- (16) Cubero, E.; Orozco, M.; Hobza, P.; Luque, F. J. *J. Phys. Chem. A* **1999**, *103*, 6394.
- (17) Liu, S. Y.; Dykstra, C. E.; Malik, D. J. *Chem. Phys. Lett.* **1986**, *130*, 403,46.
- (18) Liu, S.; Dykstra, C. E. *J. Phys. Chem.* **1986**, *90*, 3097.
- (19) Liu, S. Y.; Dykstra, C. E. *Acc. Chem. Res.* **1988**, *21*, 355.
- (20) Parish, C. A.; Dykstra, C. E. *J. Phys. Chem.* **1993**, *97*, 9374.
- (21) Masunov, A.; Dannenberg, J. J.; Contreras, R. H. *J. Phys. Chem. A* **2001**, *105*, 4737.
- (22) Interestingly, introduction of negative charge close to hydrogen atom, lead to the red shift of O–H stretching frequency in water but blue shift in C–H bonds of CH₄, CF₃H, CCl₃H. See ref 10 and Hermansson, K. *J. Chem. Phys.* **1993**, *99*, 861.
- (23) Hermansson, K. *Int. J. Quantum Chem.* **1993**, *45*, 747 for further details.
- (24) Qian, W.; Krimm, S. *J. Phys. Chem. A* **2002**, *106*, 6628.

and improper hydrogen bonds as very similar in nature. As a representative example, Scheiner and co-workers¹² have shown in a thorough study that improper and normal H-bond formation leads to similar changes in the remote parts of the H-bond acceptor, and that there are no fundamental distinctions between the mechanism of formation of improper and normal H-bonds.¹³ This is consistent with the results of AIM (“Atoms-In-Molecules”)¹⁴ analysis of Cubero et al. who found no essential differences between electron density distributions for normal and blue-shifted hydrogen-bonds.¹⁵ Several other studies which concentrate on the importance of electrostatic contributions to H-bonding and the effect of the electric field on C–H bond length support this conclusion. Earlier studies of Dykstra and co-workers were able to predict the nature of H-bonding (blue or red-shift) based on electrical moments and polarization of H-bond donors.¹⁶ Recently, Dannenberg and co-workers have shown that at small electric fields “electron density from the hydrogen moves into the C–H bond” shortening and strengthening it”,¹⁷ whereas Hermansson has modeled the electric field of H-bond acceptor with a highly accurate “electrostatic potential derived point charges” and concluded that the reasons for the blue-shift is “the sign of the dipole moment derivative with respect to the stretching coordinate combined with electronic exchange overlap at moderate and shorter H-bonded distances.”¹⁸ In a very recent paper, Li et al. suggested that X–Y bond shortening in improper H-bonding is a result of repulsive (Pauli) steric interactions between the two molecules which balance the attractive (electrostatic) forces at the equilibrium geometry.⁸ Finally, Qian and Krimm analyzed the dynamic properties of the H-bond donor group, with the particular emphasis on the force on the bond resulting from “the interaction of the external electric field created by the [proton] acceptor atom with the permanent and induced dipole derivatives of the X–H bond.” They concluded that the effect of the electric field

is more complicated such that “when the field and dipole moments are parallel, the bond lengthens, as in the case of O–H...O, when the field and dipole derivative are antiparallel, as in the case of C–H...O, the bond shortens.”¹⁹

We completely agree with those who conclude that there are no *fundamental* differences between the two types of the H-bonds and do not intend to dispute the nature of physical phenomena which were suggested to lead to bond shortening. However, in this paper, we would like to suggest a *chemical* rather than physical perspective with respect to the nature of the underlying factors controlling the direction of changes in the X–H bond length upon X–H...Y complex formation and analyze the *mechanism* of electronic reorganization by which the bond shortening occurs. This perspective is not only consistent with most of the observations and interpretations in the literature, but also it puts both types of H-bonding in the framework of classic structural organic chemistry providing chemists with a clear and unified view of this important phenomenon.

We will show that improper H-bonding is not a surprising aberration but a logical consequence of Bent’s rule,^{20,21} one of the most general rules of structural organic chemistry which predicts an increase in s-character of the X-hybrid AO of the X–H bond upon X–H...Y H-bond formation as H becomes more electropositive during this process.

Computational Details And Choice Of Method

All computations were performed using the Gaussian98 program.²² Improper H-bonding can be qualitatively described by a variety of quantum mechanical methods. Both Hartree–Fock (HF) and post-SCF methods are often able reproduce the qualitative picture (X–H bond shortening),⁸ but the MP2 method with extended basis sets is most commonly used for the description of this phenomenon, especially when accurate binding energies are required.⁷ Although all discussions in this paper are based on MP2(FC)/6-31+G* calculations, we also carried out B3LYP/6-311+G** computations on all systems in the study. The B3LYP results parallel the MP2 data quite closely and are summarized in the Supporting Information.

The changes in the electronic properties of blue-shifting (CF₃H...OH₂) and red-shifting (CF₃H...Cl[−]) complexes were analyzed by using relaxed H...Y distance scan where all geometric variables were allowed to optimize except for the (fixed) H...Y distance.

Because this paper concentrates on structural²³ rather than energetic consequences of H-bonding, in most of the complexes (especially for those structures which were reported previously) we did not correct hydrogen bond energies for the basis set superposition error (BSSE). The estimated BSSE values of several systems fall in the range of 0.05–0.25 kcal/mol. We applied BSSE corrections to the previously unknown class of blue-shifted O–H...Y complexes.²⁴

The NBO 4.0²⁵ program was used to evaluate changes in hyperconjugation, hybridization and polarization upon formation of H-bonded complexes. The NBO analysis transforms the canonical delocalized Hartree–Fock (HF) MOs, or corresponding natural orbitals of a correlated description, into localized orbitals that are closely tied to chemical bonding concepts. This process involves sequential transformation of nonorthogonal atomic orbitals (AOs) to the sets of “natural” atomic orbitals (NAOs), hybrid orbitals (NHOs) and bond orbitals (NBOs). Each of these localized basis sets is complete and orthonormal. Importantly, these sets also describe the wave function in the most “economic” way because electron density and other properties are described by the minimal amount of filled orbitals in the most rapidly convergent fashion. Filled NBOs describe the hypothetical, strictly localized Lewis structure. The interactions between filled and vacant orbitals represent the deviation of the molecule from the Lewis structure and can be used as a measure of delocalization. This method gives

- (20) An Appraisal of Valence-Bond Structures and Hybridization in Compounds of The First-Row Elements. Bent, H. A. *Chem. Rev.* **1961**, *61*, 275.
- (21) For selected applications of Bent’s rule, see: Baldrige, K. K.; Siegel, J. S. *Chem. Rev.* **2002**, *124*, 5514. Lemke, F. R.; Galat, K. J. Youngs, W. J. *Organometallics* **1999**, *18*, 1419. Kaupp, M.; Malkina, O. L. *J. Chem. Phys.* **1999**, *108*, 3648. Palmer, M. H. *J. Mol. Struct.* **1997**, *405*, 179. Palmer, M. H. *J. Mol. Struct.* **1997**, *405*, 193. Jonas, V.; Boehme, C.; Frenking G. *Inorg. Chem.* **1996**, *35*, 2097. Root, D. M.; Landis, C. R.; Cleveland, T. J. *Am. Chem. Soc.* **1993**, *115*, 4201. Kaupp, M.; Schleyer, P. v. R. *J. Am. Chem. Soc.* **1993**, *115*, 1061. Fantucci, P.; Valenti, V. *J. Chem. Soc., Dalton Trans.* **1992**, 1981. Xie, Y. M.; Schaefer, H. F.; Thrasher, J. S. *J. Mol. Struct. (THEOCHEM)* **1991**, *80*, 247. For the limitations of Bent’s rule in treating organometallic compounds see: Kaupp, M. *Chem. Eur. J.* **1999**, *5*, 3631.
- (22) Frisch, M. J.; Trucks, G. W.; Schlegel, H. B.; Scuseria, G. E.; Robb, M. A.; Cheeseman, J. R.; Zakrzewski, V. G.; Montgomery, J. A., Jr.; Stratmann, R. E.; Burant, J. C.; Dapprich, S.; Millam, J. M.; Daniels, A. D.; Kudin, K. N.; Strain, M. C.; Farkas, O.; Tomasi, J.; Barone, V.; Cossi, M.; Cammi, R.; Mennucci, B.; Pomelli, C.; Adamo, C.; Clifford, S.; Ochterski, J.; Petersson, G. A.; Ayala, P. Y.; Cui, Q.; Morokuma, K.; Malick, D. K.; Rabuck, A. D.; Raghavachari, K.; Foresman, J. B.; Cioslowski, J.; Ortiz, J. V.; Stefanov, B. B.; Liu, G.; Liashenko, A.; Piskorz, P.; Komaromi, I.; Gomperts, R.; Martin, R. L.; Fox, D. J.; Keith, T.; Al-Laham, M. A.; Peng, C. Y.; Nanayakkara, A.; Gonzalez, C.; Challacombe, M.; Gill, P. M. W.; Johnson, B. G.; Chen, W.; Wong, M. W.; Andres, J. L.; Head-Gordon, M.; Replogle, E. S.; Pople, J. A. Gaussian 98, revision A.1; Gaussian, Inc.: Pittsburgh, PA, 1998.
- (23) We also chose to not to discuss X–H stretching frequencies since they were shown (e.g., ref 8) to correlate very well with the X–H bond lengths.
- (24) We used the counterpoise (CP) correction method. Boys, S. F.; Bernardi, F. *Mol. Phys.* **1970**, *19*, 553.
- (25) NBO 4.0. Glendening, E. D.; Badenhop, J. K.; Reed, A. E.; Carpenter, J. E.; Weinhold, F. Theoretical Chemistry Institute, University of Wisconsin, Madison, WI, 1996.
- (26) Reed, A. E.; Curtiss, L. A.; Weinhold, F. *Chem. Rev.* **1988**, *88*, 899.
- (27) (a) Weinhold F. In *Encyclopedia of Computational Chemistry*; Schleyer, P. v. R., Ed.; Wiley: New York, 1998, 3, 1792. (b) See also: www.chem.wisc.edu/nbo5.
- (28) Reed, A. E.; Weinhold, F. *J. Chem. Phys.* **1985**, *83*, 1736

energies of hyperconjugative interactions both by deletion of the off-diagonal Fock matrix elements between the interacting orbitals and from the second-order perturbation approach

$$E(2) = -n_{\sigma} \frac{\langle \sigma/F/\sigma^* \rangle^2}{\epsilon_{\sigma^*} - \epsilon_{\sigma}} = -n_{\sigma} \frac{F_{ij}^2}{\Delta E} \quad (1)$$

where $\langle \sigma/F/\sigma^* \rangle$, or F_{ij} is the Fock matrix element between the i and j NBO orbitals, ϵ_{σ} and ϵ_{σ^*} are the energies of σ and σ^* NBO's, and n_{σ} is the population of the donor σ orbital.²⁶ In this paper, we used exclusively the second-order perturbation approach which provides an expedient way to estimate relative trends in hyperconjugative energies. Detailed descriptions of the NBO calculations are available.^{26,27,28}

Results and Discussion

Hydrogen bonding is a complex phenomenon and detailed analysis of *all* subtle factors involved in formation of hydrogen bonded complexes X–H...Y^{29,26,30,31} is beyond the scope of this discussion. However, we will outline the most important effects pertinent to our discussion below. The two largest stabilizing effects are (a) the hyperconjugative $n(Y) \rightarrow \sigma^*(X-H)$ interaction (which is often called “covalent component”, or “charge transfer (CT) component” because it is associated with partial electron transfer from a lone pair of atom Y, $n(Y)$, to an antibonding X–H orbital) and (b) the electrostatic interaction between inherent and induced dipoles. Destabilizing factors include the steric (exchange or Pauli) repulsion between filled orbitals and the deformation of both H-bond acceptor and H-bond donor from their optimal geometries present in the isolated species.

Because all of the above factors influence the X–H bond length in an H-bonded complex in a complex and interrelated way, a clear dissection of their relative importance can be challenging as illustrated by the ongoing discussion of the nature of improper H-bonding. We will show below that it is instructive to understand the *mechanism* of electronic and structural reorganization of X–H bonds in the process of both “proper” and “improper” H-bond formation. *This mechanism is combination of two effects: hyperconjugative X–H bond weakening and rehybridization-promoted bond X–H strengthening.* Because these two effects are general for **all** types of H-bonds, there are no fundamental differences between classical and improper H-bonding. Let us briefly outline these two factors before discussing them in more detail in the following chapter.

The importance of hyperconjugative interaction (charge transfer) from a lone pair of the H-bond acceptor to the σ^* (C–H) orbital of the H-bond donor is well-documented.²⁶ Because such interactions lead to an increase in population of an antibonding C–H orbital, they elongate the C–H bond.²⁶ Several well-known energetic and structural consequences of this effect are illustrated in Figure 1.

This hyperconjugative C–H bond weakening effect is opposed by a different effect, the importance of which, to the best of our knowledge, is not recognized. This C–H bond strengthening effect is an increase in s-character of carbon hybrid orbital in the C–H bond which occurs upon the decrease of the

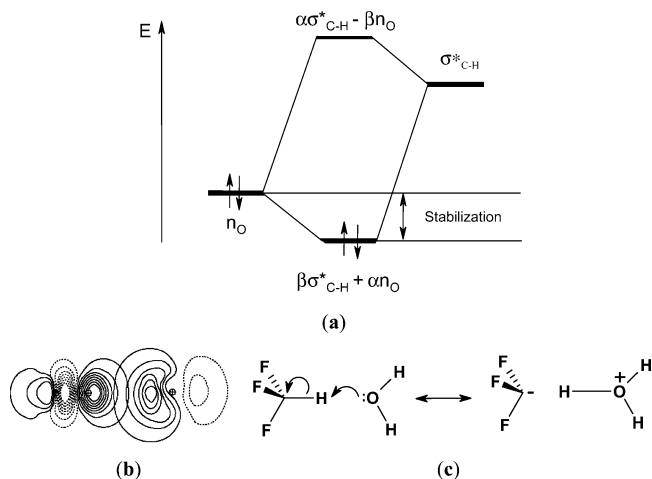


Figure 1. (a) Energy lowering due to hyperconjugative interaction between $n(Y)$ and σ^*_{C-H} orbitals in X–H...Y complex. (b) NBO plots illustrating the overlap of the σ^*_{C-H} of fluoromethane and the $n(O)$ orbital of the oxygen atom in water in the fluoromethane/water complex and (c) description of the hyperconjugative $n(O) \rightarrow \sigma^*_{C-H}$ interaction in this complex in terms of resonance theory illustrating effective charge transfer from H-bond acceptor (water) to H-bond donor (fluoromethane).

C–H...Y distance. The increase in s-character is a direct consequence of Bent’s rule—one of the most general rules governing structure of organic molecules.²⁰ According to Bent’s rule, *atoms tend to maximize the amount of s-character in hybrid orbitals aimed toward electropositive substituents and direct hybrid orbitals with the larger amount of p-character toward more electronegative substituents.* This rule illustrates the notion that hybridization of chemical bonds in organic molecules is a dynamic property aimed at maximizing chemical bonding and is highly sensitive to molecular structure and environment.³²

Hybridization as a Function of Electronegativity. Because the correlation of electronegativity with s-character is of primary importance for our model, we will analyze this correlation in some detail. We begin with considering how hybridization of an sp^n orbital on carbon in C–X bonds changes as a function of the electronegativity of X (CH₃, NH₂, OH, and F) in substituted ethanes EtX (Figure 2). As the electronegativity of X increases, so does the polarization of a C–X bond, whereas the s-character in carbon-centered hybrid atomic orbital of the C–X bond is reduced. These changes can be quite significant. For example, according to NBO analysis, the s-character of a carbon-centered hybrid orbital forming the highly polarized (75% of electron density on the fluorine atom) C–F bond is decreased and the latter is best described as an sp^4 orbital instead of the usual sp^3 orbital as in the C–H bonds of methane.

A direct consequence of Bent’s rule which is important for H-bonding is that a decrease in effective electronegativity of hydrogen in a X–H bond leads to an increase in the s-character of the carbon hybrid orbitals of this bond.³³ Such a decrease in effective electronegativity, which leads to increased bond

(29) Coulson, C. A. *Research* **1957**, *10*, 149.

(30) See for example, Morokuma, K.; Kitaura, K. In *Molecular Interactions*; Ratajczak, H., Orville-Thomas, W. J., Eds.; Wiley: New York, 1980; Chapter 2.

(31) For characterization of hydrogen bonds based on sharing of electrons in molecules. see: Fulton, R. L.; Perhaps, P. *J. Phys. Chem.* **1998**, *102*, 9001. For the sharing analysis of the behavior of electrons in some simple molecules, see: Fulton, R. L.; Perhaps, P. *J. Phys. Chem.* **1998**, *102*, 8988.

(32) On a deeper level, these two effects are connected and the rehybridization (and repolarization) itself can be considered an induced consequence of the hyperconjugative CT interaction. In lowest order, the CT interaction can be considered merely as population transfer between the fixed orbitals of (undistorted) monomers, but CT also induces higher-order orbital distortions (with associated charge reorganization) to further enhance donor–acceptor interaction. We will discuss this connection later in the paper. Another interesting way to incorporate changes in s-character in a general picture of three-center bonding is given in a recent paper: Munzarova, M. L.; Hoffmann, R. *J. Am. Chem. Soc.* **2002**, *124*, 4787–4795.

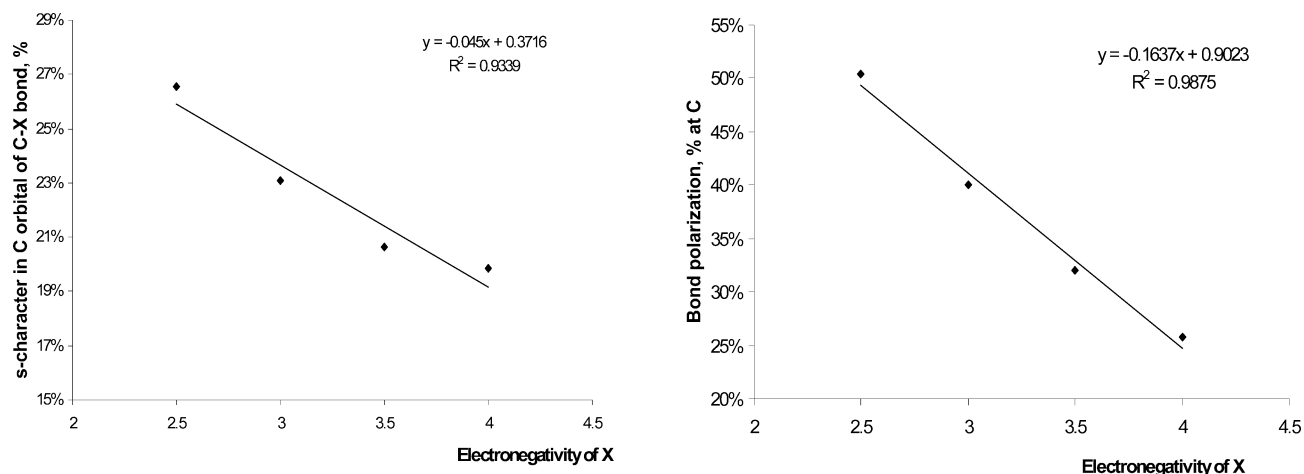


Figure 2. Correlation of s-character in C–X bonds with electronegativity of X (CH₃, NH₂, OH, and F) in substituted ethanes C₂H₅X (left) and correlation of bond polarization (% of electron density on carbon) with s-character (%) in carbon spⁿ hybrid orbital in C–X bond (MP2/6-31+G* level).

polarization, is observed when the distance between the hydrogen and a “reservoir” of electron density such as a lone pair of an H-bond acceptor is decreased. We will show below that this leads to an increase in the s-character of an X–H bond upon H-bond formation (*vide infra*). Because increase in s-character is associated with bond shortening, under certain circumstances it may counterbalance the X–H lengthening effect of the $n(Y) \rightarrow \sigma^*(X-H)$ hyperconjugative interaction. Since total s-character at any given carbon atom is conserved, an increase in the s-character in the X–H bond leads to the simultaneous increase in the p-character of other bonds connected to the central carbon atom explaining their elongation and other structural reorganizations in remote parts of the hydrogen bond donor as discussed by Hobza.⁷ However, such reorganization should be observed for all H-bonds, both classic and improper, and this is exactly what we observed in this study.

This is certainly a minimalistic model of hydrogen bonding stripped of many nuances but, surprisingly, it still captures the essence of this phenomenon and possesses predictive power needed to explain most of the experimental data regarding both proper and improper H-bonding and to predict new blue-shifted H-bonds (for example, we used it to discover the first RO–H...Y improper H-bonds, *vide infra*). The basic idea is simple: because rehybridization and hyperconjugation act in opposite directions, the observed effect of H-bonding on the bond lengths is a result of a **balance of these two intrinsic effects**. When hyperconjugation is dominant, the C–H bond lengthens. When hyperconjugation is weak and the structure of the H-bond donor allows for a significant change in C–H bond hybridization, the C–H bond shortens. In the following section, we will illustrate how this simple notion explains a number of features and trends associated with improper and classic hydrogen bonds.

C–H Bond lengths in C–H...Y Complexes as a Function of Hyperconjugation and Rehybridization. 1. Changes in C–H Bond Properties upon Approach of an H-Bond Acceptor. (A) C–H Bond Length: We start our discussion with an analysis of structural reorganization in the CHF₃ molecule as it approaches an H-bond acceptor (H₂O and Cl[−]) (known to lead to formation of an improper C–H...O hydrogen

bond in the first case and a classic H-bond in the second case). Once the nature of the underlying factors controlling C–H bond lengths is understood and differences (if any) between the two types of H-bonds are determined, we will apply these results to explain the trends in a variety of other H-bonded complexes.

To our surprise, we were not able to find any correlation of C–H bond lengths with H...Y distance in the literature except for the F₃CH...FH system recently studied by Li et al.⁸ These authors found that in the F₃CH...FH complex, the C–H bond length increases at larger distances, goes through a maximum and starts to shorten when the short-range repulsive forces come into effect. These observations were taken as evidence that bond shortening is a result of short-range repulsive effects and longer range interactions are bond lengthening. Although we were able to reproduce the above result for this particular complex, the changes in C–H bond length for CF₃H complex formation with better Lewis donors (H₂O and Cl[−]) follow a different trend. We found that in these complexes, the C–H bond continuously shortens at longer X...H distances until the σ^* (C–H) and $n(Y)$ orbitals begin to overlap directly which leads to progressive C–H bond lengthening at shorter distances. The turning point is observed earlier for the chloride anion which is consistent with the more diffuse nature of chloride lone pairs. Although the ultimate effect on the C–H bond lengths differs for the two complexes (bond shortening for Y=H₂O and C–H bond lengthening for Y=Cl[−]), in both cases the evolution of C–H distance upon decrease in X...H distance (X = O, Cl) follows a similar trend (Figure 3).

Changes in the lengths of C–F bonds (remote structural reorganization) are also evident but they follow a simpler pattern (continuous C–F bond elongation) which is qualitatively similar for both complexes (Figure 3) although some differences (such as an earlier onset and a larger C–F bond elongation for the complex with chloride) are noticeable.

(B) Hyperconjugation: The net change in the C–H bond lengths within the two complexes is different in sign only due to the differences in *relative* magnitude of the underlying factors: C–H bond lengthening in the chloride anion complex is more pronounced than in the case of the water complex. These quantitative differences are consistent with a larger role of hyperconjugative $n_p(X) \rightarrow \sigma^*(C-H)$ charge transfer (CT) interaction in the former complex due to the more spatially diffuse

(33) Increase of a hydrogen net charge is one of important criteria for the presence of H-bonding: Kock, U.; Popelier, P. L. A. *J. Phys. Chem.* **1995**, *99*, 9747. Popelier, P. L. A. *J. Phys. Chem. A* **1998**, *102*, 1873.

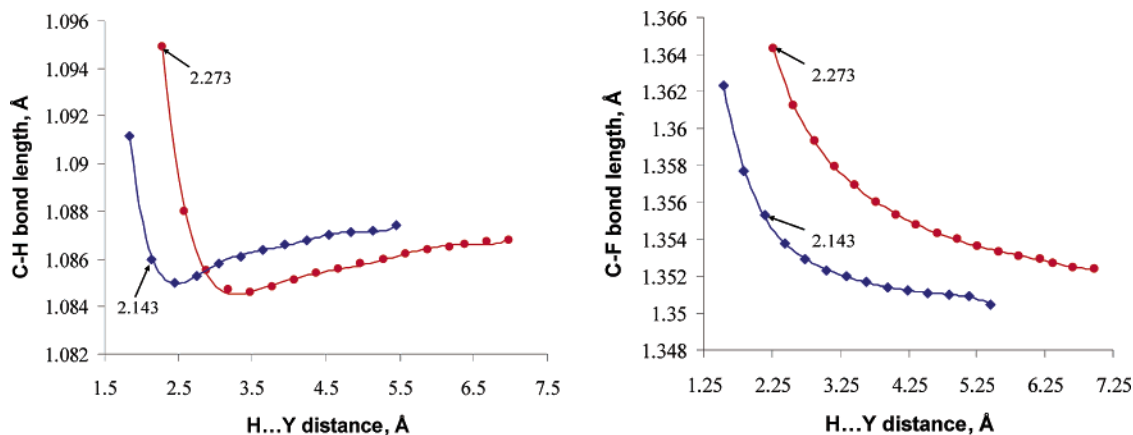


Figure 3. Correlation of C–H and C–F bond lengths with H...Y (Y = O and Cl) distance in CHF₃/water (blue diamond) and CHF₃/chloride (red circle) complexes (MP2/6-31+G* level). The equilibrium distances are shown with arrows. Here and throughout the paper all plots and data entries in blue color correspond to blue-shifted H-bonds, whereas all plots and data entries in red correspond to classic red-shifted H-bonds.

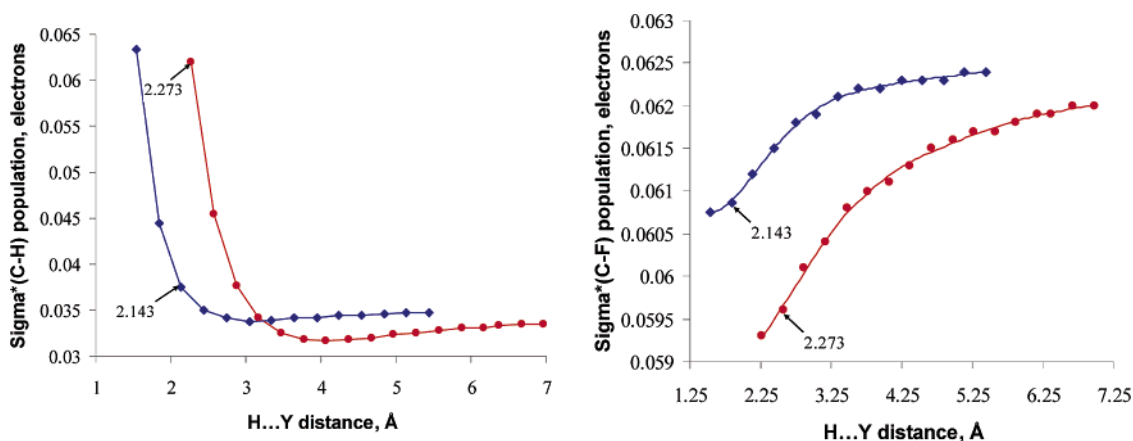


Figure 4. Correlation of population of $\sigma^*_{\text{C-H}}$ and $\sigma^*_{\text{C-F}}$ with H...Y (Y = O and Cl) distance in CHF₃/water (blue diamond) and CHF₃/chloride (red circle) complexes (MP2/6-31+G* level). The equilibrium distances are shown with arrows.

character and increased energy of nonbonding orbitals of the chloride anion compared with those of oxygen in water.

The role of hyperconjugation in H-bond formation is further illustrated by other changes in the properties of the C–H bonds. For example, at larger distances, the populations of both $\sigma^*_{\text{C-F}}$ and $\sigma^*_{\text{C-H}}$ orbitals gradually decrease (a bond-shortening effect) as both H-bond acceptors approach CHF₃.³⁴ For $\sigma^*_{\text{C-F}}$ orbitals which do not overlap with the lone pairs of H-bond acceptors, this trend is conserved even at shorter distances. The situation is different for $\sigma^*_{\text{C-H}}$ orbitals whose population starts to increase rapidly once they begin to overlap directly with the lone pair of H-bond acceptor. This makes a hyperconjugative $n \rightarrow \sigma^*$ electron-transfer possible and leads to hyperconjugative C–H bond lengthening in both blue-shifted and red-shifted CHF₃ complexes described above. Again, the similarity of the two types of H-bonding is consistent with the similar shapes of the curves for the classic and improper H-bonds in Figure 4.

The magnitude and distance (overlap) dependence of hyperconjugative contributions to H-bonding can be obtained from NBO energetic analysis.²⁶ The trends in interaction energies given in Figure 5 indicate that at distances below 2.8–3.5 Å

the increased orbital overlap leads to increase in the importance of hyperconjugation. This region almost coincides (although with a short delay) with the onset in C–H bond lengthening in both CHF₃/water and CHF₃/chloride anion complexes. Importantly, combined analysis of Figure 3a and Figure 5 determines the threshold (which corresponds to second-order perturbation energy for $n(\text{Y}) \rightarrow \sigma^*(\text{H-X})$ interaction in the order of 3–5 kcal/mol) at which the bond-lengthening effect of hyperconjugative interactions overcomes the bond-shortening effects. This estimate is certainly approximate and will vary depending on the nature of the H-bond donor and H-bond acceptor but, as we will show below, the magnitude of this threshold determines the borderline between systems exhibiting improper and proper H-bonding for the majority of systems discussed in this paper.

(C) Rehybridization/Repolarization: The second group of changes involves C–H bond shortening effects. As evident from Figure 3, although these effects are dominant at larger H...Y distances, usually (in a classic H-bond) they become partially overshadowed by hyperconjugation at shorter distances. The situation is different for improper H-bonds.

The first C–H bond shortening effect is due to the increase in C–H bond polarization upon H-bond formation (Figure 6). This increase is echoed in the increase of positive charge on hydrogen, decrease of positive charge on carbon and increase of negative charge on fluorine. The latter group of changes is reflective of a decrease in effective electronegativity of the

(34) Decrease in population of $\sigma^*_{\text{C-H}}$ orbitals is consistent with shift of electron density from hydrogen in the C–H bond (repolarization of the bond). Because, σ^* has larger coefficient on hydrogen, such electron density shift decreases the population of this orbital.

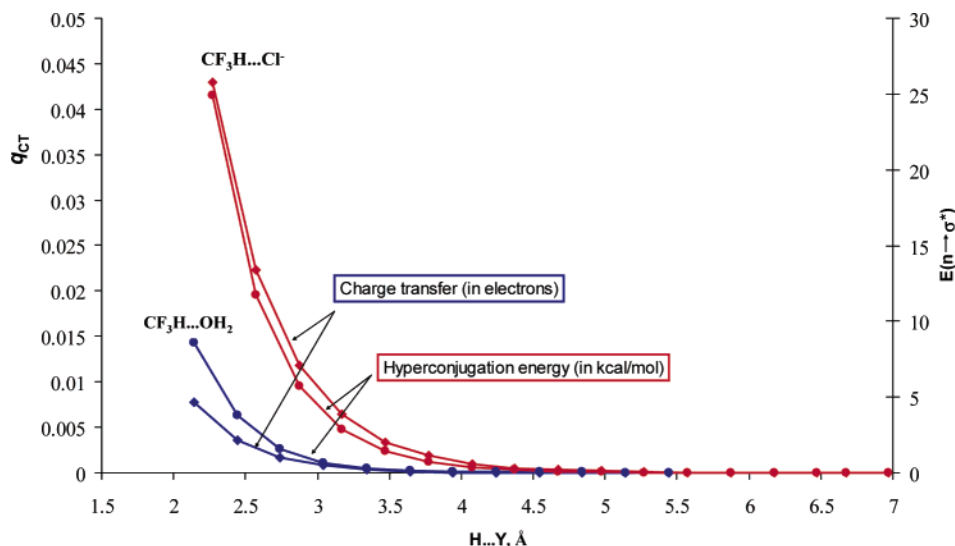


Figure 5. Correlations of both charge transfer (diamond) and energy of $n(X) \rightarrow \sigma^*(C-H)$ interactions (circle) with $H \dots Y$ distance in CHF_3 /water (blue) and CHF_3 /chloride (red) complexes (MP2/6-31+G* level).

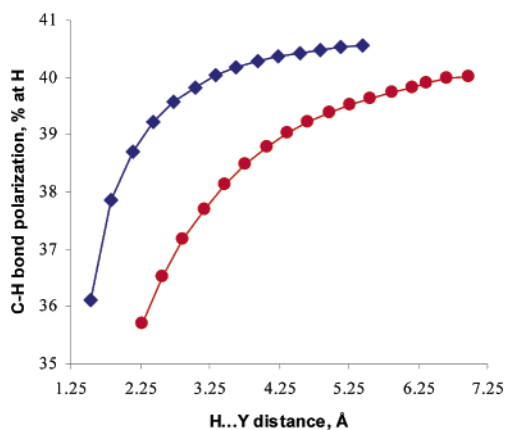


Figure 6. Correlation of $\sigma(C-H)$ polarization (% of electron density at hydrogen) with $O \dots H$ distance in CHF_3 /water (left) and CHF_3 /chloride (right) complexes.³⁶ (MP2/6-31+G* level).

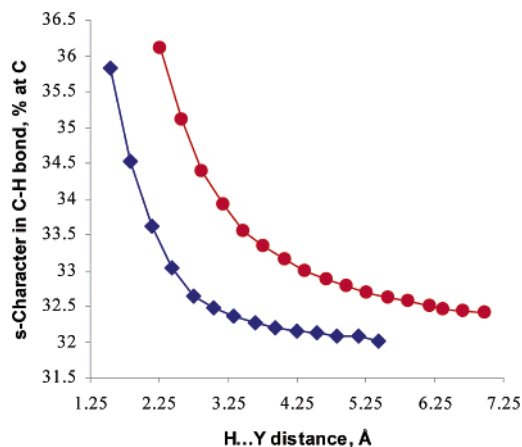


Figure 7. Correlation of s -character in $\sigma(C-H)$ bonds (%) with $O \dots H$ distance in CHF_3 /water (left) and CHF_3 /chloride (right) complexes. (MP2/6-31+G* level).

hydrogen atom which, in excellent agreement with Bent's rule, leads to an increase in the s -character in the carbon hybrid orbital forming the $C-H$ bond effect which should lead to $C-H$ bond shortening.³⁵ Because the total s -character on the central carbon atom is conserved, an increase in the s -character of the $C-H$

bond leads to a simultaneous increase in p -character in the three $C-F$ bonds which results in their lengthening as observed by Hobza (Figures 7 and 8).⁷

Figure 9 illustrates that bond polarization³⁷ and rehybridization are highly correlated for both CHF_3 /water (left) and CHF_3 /chloride scans. At longer distances the data points for both complexes can be combined into one curve which suggests that the nature of long-range effects is similar in these two cases. As the systems approach to the equilibrium $H \dots Y$ distance, the percentage of s -character starts to increase even faster than the polarization of $C-H$ bond toward carbon which explains the observed divergence of corresponding trends for the two complexes in Figure 9.

(D) Connection between Rehybridization/Repolarization and Hyperconjugative Charge Transfer (CT) Interactions: It is important to further emphasize that the rehybridization (and repolarization) itself can be considered an induced consequence of the hyperconjugative CT interaction. In the lowest order approximation, the CT interaction can be considered merely as population transfer between the fixed orbitals of (undistorted) monomers, but CT also induces higher-order orbital distortions (with associated charge reorganization) to further enhance donor-acceptor interaction. The repolarization of σ^* ($X-H$) toward H (σ toward X) has the double benefit of amplifying the $n \rightarrow \sigma^*$ interaction while reducing the $n-\sigma$ interaction (steric repulsion), both increasing net attraction. Repolarization becomes easier (and the charge reorganization more pronounced) as the electronegativities of X and H become more equal, whereas the effect diminishes when $\sigma(X-H)$ is already highly polar. The CT-induced repolarization has the superficially paradoxical effect of reducing net electron density at H (even

(35) Increased polarity (ionic character) of the $C-H$ bond also should lead to $C-H$ bond shortening. Note that a similar observation of increased polarization and s -character has been made by Kryachko, E. S.; Zeegers-Huyskens, T. *J. Phys. Chem. A* **2002**, *106*, 6832, by Li et al. in ref 8 and possibly by others.

(36) A typical s bond $C-X$ can be described as: $\sigma_{C-X} = \alpha(sp^n)_C + \beta(sp^m)_X$ where α and β are polarization coefficients for the C - and X -centered hybrids $(sp^n)_C$ and $(sp^m)_X$. α_2 and β_2 are proportional to electron density at the C - and X -hybrids with $\alpha_2 + \beta_2 = 1$. When X is more electronegative than C, $\alpha_2 > 0.5 > \beta_2$.

(37) Note that increase in the ionic character of $C-H$ bond is an additional factor leading to shortening of this bond.

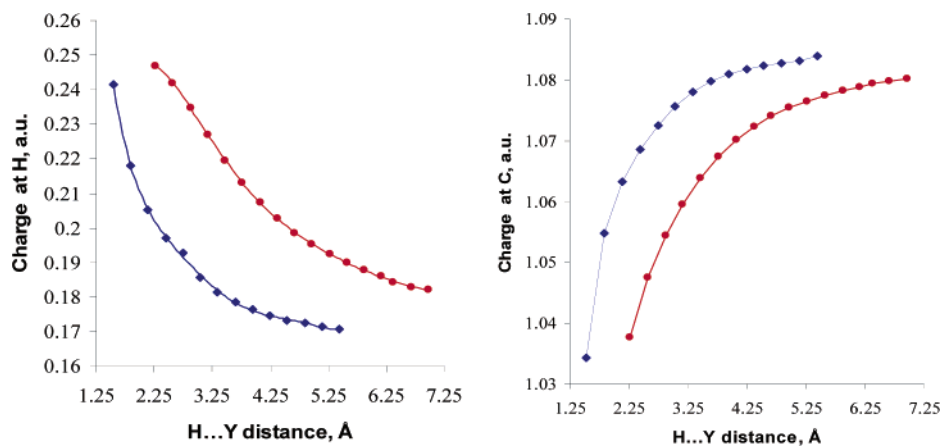


Figure 8. Correlation of population of charges H and C in C-H bond with H...Y (Y = O and Cl) distance in CHF₃/water (blue diamond) and CHF₃/chloride (red circle) complexes (MP2/6-31+G* level).

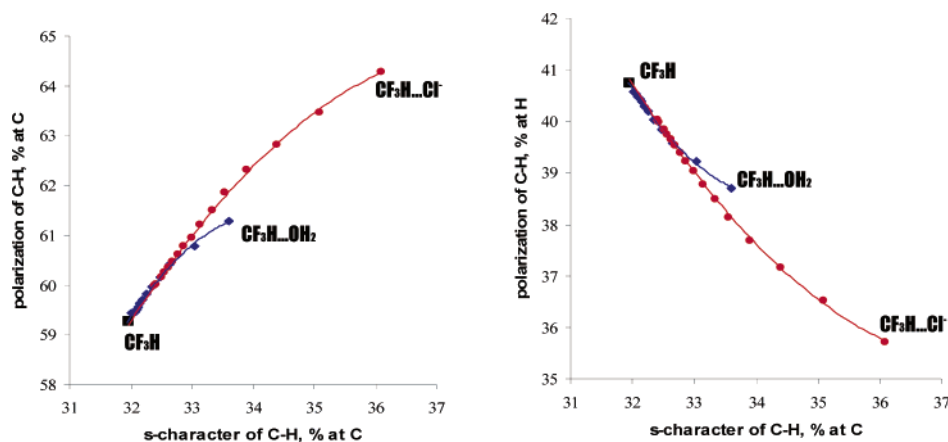


Figure 9. Combined correlation of polarization of C-H bond and percent of s-character at C-centered hybrid in this bond for all scanned distances in CHF₃/water (blue diamond) and CHF₃/chloride (red circle) complexes (MP2/6-31+G* level).

though charge was transferred into a σ^* orbital with greater amplitude at H), and it leads to the Bent's Rule shifts in hybridization which we have quantified above. Thus, the whole collection of effects bears the signature of strong correlation with the strength of the $n-\sigma^*$ CT interaction “driving force”, with proportionality to intrinsic X-H bond polarizability ($\chi(X) - \chi(H)$ electronegativity difference).

Despite the different equilibrium C-H bond lengths in the two complexes, the nature of changes which accompany the formation of both of the complexes is very similar for “classic” and “improper” H-bonding. The only difference is in the relative magnitude, or *balance*, of the different factors. In the absence of dominating hyperconjugative interactions, the relative role of other relatively subtle effects such as dispersion forces may increase as previously suggested by Hobza,⁷ but the qualitative pictures of improper and proper H-bonding are similar as noted recently by other researchers.^{8,9,10,13,17}

(E) Sensitivity of C-H Bond Length to Changes in Hybridization. The next question is whether the changes (from $sp^{2.12}$ to $sp^{1.97}$) in the s-character of C-H bonds are sufficient to explain the C-H bond shortening. The sensitivity of C-H bond lengths to changes in s-character can be estimated from the values of experimental C-H bond lengths in ethane, ethylene and acetylene³⁸ which are illustrated in Figure 10. Comparison of these data with the calculated C-H bond lengths

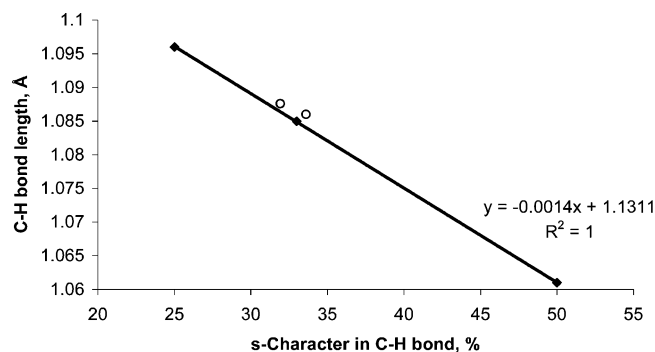


Figure 10. Correlation of s-character in the carbon hybrid orbitals of C-H bonds with the experimental C-H bond lengths in ethane, ethylene and acetylene (diamonds, the s-character is taken as 33%, 25%, and 50% respectively) in comparison with MP2/6-31+G* computed lengths and the s-character of C-H bonds in isolated fluoroform and its complex with water (hollow circles).

in fluoroform and its complex in water suggests that the change in C-H bond hybridization is indeed sufficient to explain the C-H bond shortening (we will discuss the validity of this assumption for other H-bond acceptors in one of the following chapters).

Not surprisingly, the changes in electronic structure of different parts of the CF₃H molecule are highly correlated and the increase in positive charge on hydrogen is accompanied by a simultaneous increase in the negative charges on carbon and fluorine atoms. Approximately half of electron density which

(38) Delley, B. J. *Chem. Phys.* **1991**, *94*, 7425.

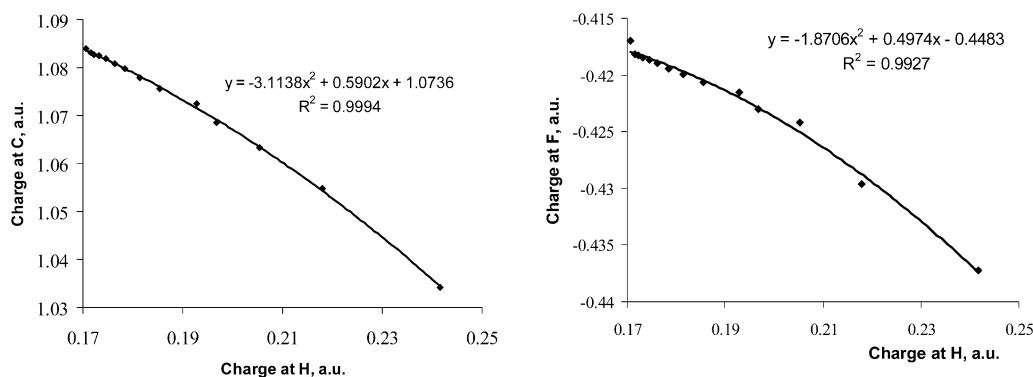


Figure 11. Correlation of natural charges of carbon and hydrogen atoms (left) and fluorine (average) and hydrogen atoms (right) during O...H distance scan in CHF₃/water complex (MP2/6-31+G* level).

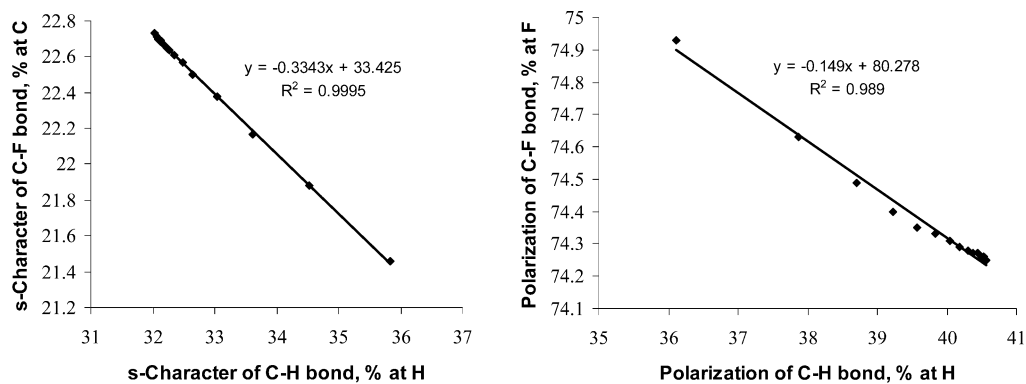


Figure 12. Correlation of changes in hybridization (left) and polarization (right) of C–H bond and C–F bond during O...H distance scan in CHF₃/water complex. (MP2/6-31+G* level).

is displaced from hydrogen moves to carbon while the rest is equally distributed between the three fluorine atoms (Figure 11). A similar correlation is observed for the changes in polarization and hybridization of C–H and C–F bonds Figure 12. This explains changes in the remote parts of the molecule such as in C–F bonds and fluorine lone pairs which are certainly integral parts of the detailed picture of the F₃CH...Y complexes formation.⁷

(F) Conclusions from the Above Analysis. A first conclusion from the above analysis is that improper H-bonding is likely to be observed only when the X–H bond elongating hyperconjugative $n(Y) \rightarrow \sigma^*(X-H)$ interaction is relatively weak.³⁹ Therefore, it is not surprising that other weak σ -acceptors such as Si–H and P–H bonds also display improper H-bonding behavior as shown recently by Schlegel and co-workers.⁸ We will show below that the X–H bond lengths in the new types of X–H...Y improper H-bonds are also controlled by the same effects as in the case of C–H bonds.

The second conclusion is that, in order for improper H-bonding to occur, the molecular structure should allow significant rehybridization of the X–H bond upon formation of the complex. If molecular structure inhibits rehybridization, then red-shifted H-bonding will be observed even for X–H bonds with relatively weak hyperconjugative σ -acceptor ability (vide infra). Certainly, a larger rehybridization will be needed to compensate for the presence of stronger hyperconjugative interactions, whereas smaller rehybridization will suffice when hyperconjugation is extremely weak. However, in both cases rehybridization is needed, and we will show that molecules

which are not able to undergo efficient rehybridization do not exhibit improper H-bonding.

2. Influence of Electronic Properties of H-Bond Acceptors on C–H Bond Lengths in C–H...Y Complexes. We tested the first conclusion by changing the relative magnitude of hyperconjugative $n(Y) \rightarrow \sigma^*(C-H)$ interactions in C–H...Y H-bonds by varying the H-bond acceptors Y. This was achieved in different complexes of CF₃H (an H-bond donor which is known to exhibit both classic and improper H-bonding) with anionic (F[−], Cl[−]) inorganic, neutral inorganic (FH, ClH, H₂O, H₂S, NH₃) and organic (oxirane, benzene and pyridine) H-bond acceptors. For pyridine both σ - and π -complexes were studied. The continuous changes in the balance of hyperconjugation and rehybridization provided by this series allowed a better understanding of the role of H-bond acceptors in improper H-bonding.

The structural, electronic and energetic parameters pertinent to formation of H-bonded complexes with these H-bond acceptors are listed in Table 1. Lengths of C–H bonds display significant variations (from -0.0032 to $+0.0405$ Å relative to the value of 1.0876 Å in isolated CHF₃ molecule) depending on the H-bond acceptor. In general, the magnitude of hyperconjugative interactions $n(Y) \rightarrow \sigma^*(C-H)$ is the most important factor in defining the C–H bond length (Figure 13). As expected, anionic lone pairs are considerably better electron donors than their neutral counterparts, and the relative trends in hyperconjugative donor ability of the H-bond acceptors can be readily understood based on the relative energies of non-bonding donor orbitals and their overlap with the acceptor σ^* -(C–H) orbitals.

(39) Alabugin I. V.; Zeidan, T. A. *J. Am. Chem. Soc.* **2002**, *124*, 3175.

Table 1. NBO Analysis of Improper H-bonding Complexes of CF₃H with Various H-bond Acceptors (F⁻(1), FH (2), Cl⁻ (3), ClH (4), H₂O (5), H₂S (6), NH₃(7), Me₂O (8a), Oxirane (8b)) Calculated from MP2/6-31+G* Calculations along with the Interaction Energies (kcal/mol)

parameter ^a	CF ₃ H	(1)	(2)	(3)	(4)	(5)	(6)	(7)	(8a)	(8b) ^b
C-H, Å	1.0876	1.1281	1.0856	1.0949	1.0861	1.0860	1.0863	1.0888	1.0867	1.0844
Δr ^a	-	0.0405	-0.0020	0.0073	-0.0015	-0.0016	-0.0013	0.0012	-0.0009	-0.0032
C-F, Å	1.351	1.375	1.353	1.364	1.351	1.355	1.353	1.357	1.356	1.353
H...Y, Å	-	1.583	2.266	2.273	2.776	2.143	2.788	2.234	2.123	2.337
q _C	1.085	0.994	1.074	1.038	1.076	1.063	1.070	1.056	1.061	1.072
q _H	0.167	0.322	0.187	0.247	0.177	0.205	0.183	0.212	0.204	0.195
q _F	-0.417	-0.460	-0.422	-0.443	-0.419	-0.426	-0.421	-0.428	0.425	0.423
q _{CT}	-	0.064	0.003	0.043	0.006	0.008	0.010	0.015	0.011	0.007
n(σ _{CH})	1.9914	1.9924	1.9914	1.9932	1.9917	1.9914	1.9918	1.9918	1.9907	1.9911
n(σ _{CF})	1.9954	1.9943	1.9954	1.9949	1.9954	1.9953	1.9954	1.9953	1.9953	1.9952
n(σ* _{CH})	0.0351	0.0765	0.0351	0.0619	0.0388	0.0375	0.0414	0.0429	0.0404	0.0353
n(σ* _{CF})	0.0625	0.0587	0.0618	0.0593	0.0618	0.0612	0.0615	0.0609	0.0601	0.0623
n(Lp _Y)	-	2.0000	2.0000	2.0000	1.9997	1.9998	2.0000	1.9997	1.9763	1.9925
n(Lp _Y) _{X,Y}	-	1.9372	1.9969	1.9574	1.9938	1.9910	1.9898	1.9837	1.9667	1.9899
spn (CH)	sp2.12	sp1.60	sp2.05	sp1.76	sp2.06	sp1.97	sp2.03	sp1.93	sp1.96	sp2.01
% s-char	31.92	38.28	32.82	36.11	32.56	33.6	32.91	34.07	33.66	33.10
spn (CF)	sp3.37	sp3.81	sp3.42	sp3.65	sp3.42	sp3.48	sp3.43	sp3.51	sp2.49	sp3.47
% s-char	22.79	20.72	22.48	21.43	22.52	22.21	22.42	22.04	22.17	22.25
pol C% (σ _{CH}), H%	59.3	68.6	60.3	64.3	59.9	61.3	60.3	61.8	61.3	60.7
pol C% (σ _{CF}), F%	40.7	31.4	39.7	35.7	40.1	38.7	39.7	38.2	38.7	39.3
pol C% (σ _{CF}), F%	25.8	24.2	25.6	24.9	25.7	25.5	25.7	25.4	25.6	25.4
E(n→σ*)	-	54.0	3.6	24.9	4.6	8.6	6.6	11.7	8.5	2.0
ΔE _{int}	-	27.1	2.6	16.6	1.8	5.2	2.8	6.1	5.5	5.7

^a Average values are used for the unsymmetrical systems. ^b There are three blue-shifting H-bonds in this complex. ^c The difference in the C–H distance between the monomer and complex. The C–H lengths in the blue-shifted complexes are shown in blue, the C–H lengths in the red-shifted complexes are shown in red.

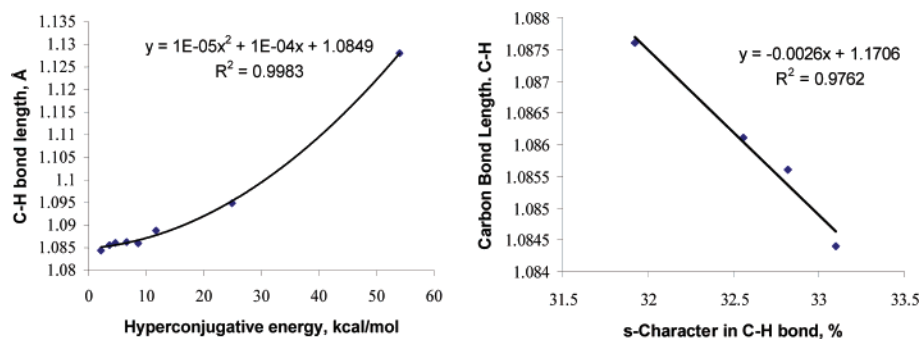


Figure 13. Correlation of C–H bond length with energy of $n(Y) \rightarrow \sigma^*(C-H)$ hyperconjugative interactions (on the left) in all F₃CH...Y complexes and with s-character at C-hybrid orbital of C–H bond (on the right). For the second correlation only the values for the isolated fluoroform molecule and the three cases when energy of $n(X) \rightarrow \sigma^*(C-H)$ interaction < 5 kcal/mol (Y=FH, ClH, oxirane) were used (MP2/6-31+G* level).

Hybridization of the C–H bond in fluoroform is also remarkably sensitive to the environment and changes from sp^{1.6} to sp^{2.12} in different H-bonded complexes. Nevertheless, as expected, there is no apparent *global* correlation between s-character in C–H bonds and C–H bond lengths for all H-bondacceptors in Table 1 and Table 2. This is due to the dominating effect of hyperconjugation-induced CT bond lengthening in most of the complexes (Figure 13). In fact, in the case of strong electron donors where the $n(Y) \rightarrow \sigma^*(C-H)$ component is large (energy > 11 kcal/mol), the effect of rehybridization is completely overshadowed by CT bond lengthening. As a result, an increase in the C–H bond lengths is observed

compared with the isolated CF₃H molecule.⁴⁰ However, the situation is different for those cases when hyperconjugation is weak (Y=FH, ClH, oxirane where the energy of the $n(Y) \rightarrow \sigma^*(C-H)$ interaction is less than the 5 kcal/mol threshold). Figure 13b illustrates that for such cases the observed C–H bond lengths indeed correlate well with s-character in the corresponding C–H bonds.

Even though changes in s-character lead to improper H-bonding only for a minor fraction of the complexes where their effect is not overshadowed by hyperconjugation, there is still an excellent global correlation (Figure 14) between C–H bond polarization and s-character which is valid for *all* H-bonded

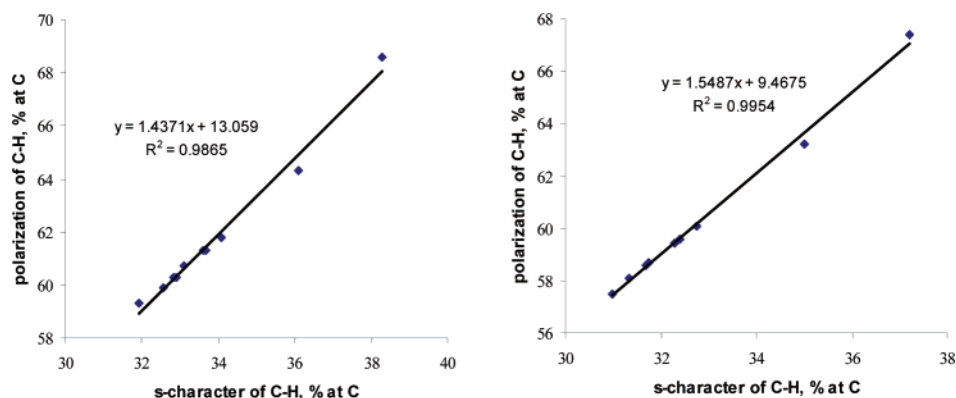


Figure 14. NBO polarizations of C–H bonds versus change in s-character calculated at the MP2/6-31+G* (left) and B3LYP/6-311+G** (right) levels.

Table 2. NBO Analysis of Improper H-Bonding Complexes of CF₃H (X) with Benzene and Pyridine Computed at the MP2/6-31+G* Level along with the Interaction Energy (kcal/mol)

parameter	CF ₃ H			
C–H, Å	1.0876	1.0880	1.0873	1.0886
Δr ^a	-	0.0004	-0.0007	0.0006
C–F, Å	1.351	1.354	1.353	1.350
H...Y, Å	-	2.672	2.783	2.240
q _C	1.085	1.075	1.076	1.058
q _H	0.167	1.085	0.179	0.185
q _F	-0.417	-0.422	-0.419	-0.426
q _{CT}	-	0.006	0.002	0.012
n(σ _{CH})	1.9914	1.9923	1.9918	1.9909
n(σ _{CF})	1.9954	1.9953	1.9953	1.9953
n(σ* _{CH})	0.0351	0.0350	0.0360	0.0415
n(σ* _{CF})	0.0625	0.0612	0.0619	0.0610
spn (CH)	sp2.22	sp1.98	sp2.02	sp1.94
% s-character	30.97	33.46	32.97	33.88
spn (CF)	sp3.29	sp3.47	sp3.45	sp3.50
% s-character	23.19	22.23	22.33	22.09
pol (σ _{CH}), C%	57.5	60.2	59.9	61.6
H%	42.5	39.8	40.1	38.4
pol (σ _{CF}), C%	28.0	25.6	25.7	25.5
F%	72.0	74.4	74.3	74.5
E(n(or π) → σ*)	-	3.6	2.4	9.8
ΔE _{int}	-	5.6	4.4	5.7

^a The difference in the C–H distance between the monomer and complex.

complexes (both classic and improper) considered above (note the similarity to the plot in Figure 2).

The presence of *several* intermolecular contacts is an additional feature of some of the H-bonded complexes. Although this complicates the general picture somewhat and makes global correlations for these complexes less meaningful, it is also an interesting phenomenon by itself. The most interesting example is provided by the complex of fluoroform with oxirane (Figure 15).⁴¹ In addition to the C–H...O hydrogen-bond, there are two C–H...F attractive interactions. Note that *all* three C–H-bonds involved into these interactions are shortened and thus this strongly bound complex (binding energy of 5.7 kcal/mol) is triply improper! Complete structures of all complexes are given in the Supplementary section and are outlined in Figure 16

(40) Note, however, that hyperconjugation provides considerable portion of the binding energy for other complexes too (even when its effect on the C–H bond length is counterbalanced by the effect of rehybridization). In fact, the second-order perturbation estimate shows that in several cases the hyperconjugation energy is larger than the binding energy. There is no hidden contradiction here because the binding energy consists of several attractive (hyperconjugative, electrostatic) and repulsive (steric, deformation) components.

(41) Cubero, E.; Orozco, M.; Lague, F. J. *Chem. Phys. Lett.* **1999**, *310*, 445.

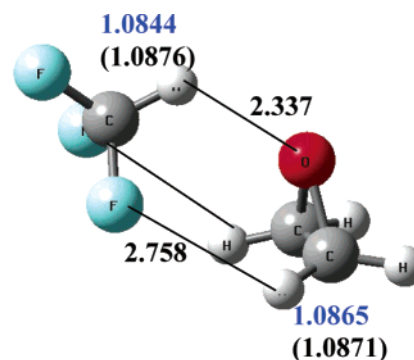


Figure 15. MP2/6-31+G* optimized structure of CF₃H...oxirane complex with the multiple blue shifted hydrogen bonds. The C–H bond lengths in the monomers are given in parentheses.

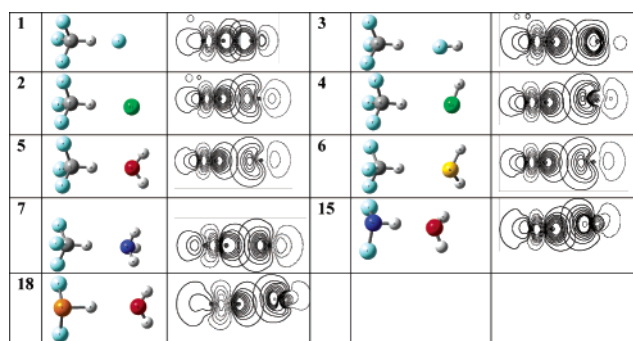


Figure 16. MP2/6-31+G* optimized geometries of hydrogen bonded XH...Y complexes (X = CF₃H, NF₂H, and PF₂H, Y = F⁻, HF, Cl⁻, HCl, H₂O, and H₂S, NH₃) and NBO contour diagrams showing the dominant hyperconjugative interaction ($n_Y \rightarrow \sigma^*_{CH}$) for the corresponding complexes.

(along with the pertinent orbital plots for the hyperconjugative $n(Y) \rightarrow \sigma^*(C-H)$ interactions). Note that the geometry is far from optimal collinear arrangement of $n(O)$ and $\sigma^*(C-H)$ orbitals and this complex trades one strong hyperconjugative interaction for three weaker contacts.

The above interesting features notwithstanding, the situation for the majority of complexes is more straightforward. All complexes 1–7 display geometries with classic H-bonding directionality (almost collinear geometry for the C–H...Y triade) and a single dominant hyperconjugative $n_Y \rightarrow \sigma^*_{CH}$ orbital interaction (Figure 16).

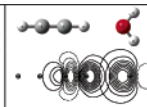
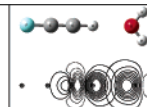
Another interesting trend is illustrated in Table 2 where three complexes with very similar stabilization energies show either classic or improper behavior as a result of a subtle balance of the several factors discussed earlier. As evident from the

magnitude of total charge transfer (q_{CT}), the hyperconjugative donation from the π -system of the electron acceptor pyridine ring is one-third than that of the benzene π -system, which explains why there is no C–H bond elongation in the π -pyridine complex. In contrast to the pyridine π -system, the pyridine nitrogen lone pair is a good hyperconjugative donor. As a result, noticeable C–H bond elongation is observed in the σ -complex of pyridine and fluoroform.

3. Influence of Electronic Properties of H-Bond Donors on X–H Bond Lengths in X–H...Y Complexes. (A) Inhibition of Improper Behavior by a Change in the Ability of X–H Bonds to Rehybridize. The electronic properties of H-bond donors are equally important in determining whether a classic or improper type of H-bond is observed. The above analysis suggests that there are two ways by which properties of H-bond donors can decrease the probability of improper behavior. The first way includes use of strong σ -acceptors capable of participating in strong hyperconjugative interactions. The second less common way is to change the ability of X–H bonds to adjust their hybridization upon formation of the complex. The role of this factor is illustrated by the literature which describes different trends in H-bonding in C–H...Y systems depending on the original hybridization of C–H bonds. For example, Scheiner and co-workers reported that the improper character in C–H...Y H-bonds is weakened in sp^2 C–H bonds compared with sp^3 C–H bonds. The trend is further enhanced for sp -hybridized C–H bonds which show only classic H-bonding patterns.^{12a} These findings were confirmed in a thorough study by Radom and co-workers.⁴² Hobza and Havlas reported a similar effect for the complexes of benzene with $CHCl_3$ and HCN .⁷ They noted that although acidities and charges on hydrogen are comparable in both cases, C–H bonds in these two cases respond differently to complex formation: a blue-shifted complex is formed with the sp^3 C–H bond in $CHCl_3$ whereas a classic red-shifted H-bond formation was observed with the sp C–H bond in the HCN complex. A similar observation was reported by Dannenberg and co-workers who found that the C–H bond in methane contracts but the C–H bond in acetylene elongates when external electric field is applied.¹⁷

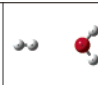
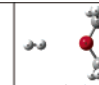
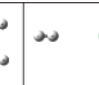
In the next section, we will show how the above observations are readily explained by the relative susceptibility of different C–H bonds to rehybridization. For this purpose, we have analyzed complexes of $FC\equiv CH$ and acetylene with water and found that the relative changes in hybridization upon formation of H-bonds are less pronounced in these systems when compared with similar complexes involving sp^3 - and sp^2 hybridized C–H bonds. The increased stiffness of acetylenic C–H bonds can be explained as a result of fixed hybridization of two out of four orbitals at the sp carbon.⁴³ Because of that, any increase in s -character of an sp C–H bond should be compensated by a decrease in the s -character and lengthening of the rather stiff $C\equiv C$ bond. As the result, relative changes in hybridization are smaller for sp C–H bonds than for their sp^3 cousins. For example, the hybridization of the C–H bond in CHF_3 changes from $sp^{2.12}$ to $sp^{1.97}$ (i.e., from 32.1% to 33.7% s -character) while the hybridization of the C–H bond in $FC\equiv CH$ changes only

Table 3. NBO Analysis of the H-bonded Complexes of $HC\equiv CH$ and $FC\equiv CH$ with H_2O at the $MP2/6-31+G^*$ Level

	$HC\equiv CH$		$FC\equiv CH$	
C–H, Å	1.0676	1.0723	1.0660	1.0716
Δr^a	-	0.0047	0.0026	0.0056
H...O, Å	-	2.141	-	2.141
q_C	-0.250	-0.239	-0.411	-0.404
q_H	0.250	0.271	0.262	0.284
q_{CT}	-	0.009	-	0.009
$n(\sigma_{CH})$	1.9897	1.9880	1.9856	1.9840
$n(\sigma^*_{CH})$	0.0057	0.0131	0.0048	0.0135
$n(O_{LP})$	1.9998	1.9914	1.9998	1.9906
sp^n (CH)	$sp^{1.05}$	$sp^{1.02}$	$sp^{0.96}$	$sp^{0.92}$
% s -character	48.60	49.54	51.00	51.99
pol (σ_{CH}), C%	62.5	63.8	63.0	64.4
H%	37.5	36.2	37.0	35.6
$E(n \rightarrow \sigma^*)$	-	7.1	-	8.1
ΔE_{int}	-	5.6	4.4	5.7

^a The difference in the C–H distance between the monomer and complex.

Table 4. NBO Analysis of the $H_a-H_b \dots Y$ ($Y = H_2O, OMe_2,$ and Cl^-) Complexes

Parameter	H_2			
		(29)	(30)	(31)
H_a-H_b , Å	0.7375	0.7389	0.7395	0.7483
Δr^a	-	0.0014	0.0020	0.0008
$H_b \dots Y$, Å	-	2.680	2.681	2.932
q_{H_a}	0.000	-0.0300	-0.0295	-0.0873
q_{H_b}	0.000	0.0287	0.0266	0.0798
q_{CT}	-	0.0013	0.0029	0.0075
$n(\sigma_{HH})$	1.9981	1.9996	1.9981	1.9999
$n(\sigma^*_{HH})$	0.0038	0.0016	0.0038	0.0071
$n(L_{py})$	-	1.9998	1.9763	2.0000
$n(L_{py})_{complex}$	-	1.9982	1.9702	1.9925
pol, H_a %	50.00	51.5	51.4	54.2
(σ_{HH}) , H_b %	50.00	48.5	48.6	45.8
$E(n \rightarrow \sigma^*)$	-	1.22	1.51	3.26
ΔE_{int}	-	0.47	0.62	2.36

^a The difference in the H–H distance between the monomer and complex.

from $sp^{0.96}$ to $sp^{0.92}$ (i.e., from 51.0% to 52.1% s -character) upon formation of complexes of these two fluorocarbons with water. In addition, $sp \sigma^*(C-H)$ orbitals are, in general, better hyperconjugative acceptors than $sp^3 \sigma^*(C-H)$ orbitals because they have lower energy and more favorable polarization of $\sigma^*(C-H)$ toward H, which should increase the magnitude of C–H bond lengthening $n(Y) \rightarrow \sigma^*(C-H)$ interactions in the case of acetylenic C–H bonds. These combined factors explain why the blue shift decreases when going from sp^3 to sp^2 hybridized carbons and is not observed at all at sp hybridized carbons.⁴⁴

Probably, the ultimate example of a bond which is not capable of rehybridization is the H–H bond.⁴⁵ According to our model, formation of H–H...Y complexes should always lead to the red-shift even though the σ^*_{HH} orbital is a relatively weak acceptor and energies of the corresponding $n(Y) \rightarrow \sigma^*_{HH}$ interactions are below the 3–5 kcal/mol threshold. This notion is an excellent agreement with the computational results reported in Table 4. All H–H...Y complexes are red-shifted!

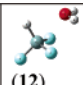

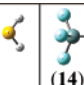
(42) Wetmore, S. D.; Schofield, R.; Smith, D. M.; Radom, L. *J. Phys. Chem. A* **2001**, *105*, 4470.

(43) These are pure p -orbitals forming the π -bonds.

(44) Cyclic systems are also less free to alter hybridization (due to constraints of ring geometry) and thus might also exhibit similar exceptions.

(45) This idea was provoked by a comment of an anonymous referee to whom we are grateful.

Table 5. NBO Analysis on the Improper H-bonded Complexes of SiF₃H (X) with H₂O, H₂S and NH₃ at MP2/6-31+G* Level^b

	SiF ₃ H	 (12)	 (13)	 (14)
Si-H, Å	1.4591	1.4547	1.4572	1.4571
Δr ^a	-	0.0044	0.0019	0.0020
Si-F, Å	1.605	1.611	1.606	1.610
H...Y, Å	-	2.671	3.195	2.647
q _{Si}	2.418	2.414	2.407	2.386
q _H	-0.310	-0.295	-0.297	-0.270
q _F	-0.703	-0.710	-0.704	-0.707
q _{CT}	-	0.016	0.002	0.005
n(σ _{SiH})	1.9670	1.9667	1.9660	1.9639
n(σ _{SiF})	1.9903	1.9901	1.9903	1.9903
n(σ* _{SiH})	0.0406	0.0404	0.0418	0.0426
n(σ* _{SiF})	0.0564	0.0592	0.0564	0.0565
n(LP _Y)	-	1.9998	2.0000	1.9997
n(LP _Y) _{complex}	-	1.9828	1.9973	1.9937
spn (SiH)	sp2.26	sp2.17	sp2.23	sp2.16
% s-character	29.56	30.53	29.94	30.62
spn (SiF)	sp3.12	sp3.18	sp3.14	sp3.18
% s-character	23.53	23.20	23.40	23.19
pol (σ _{SiH}), Si% H%	34.1 65.9	34.9 65.1	34.8 65.2	36.1 63.9
pol (σ _{SiF}), Si% F%	11.3 88.7	11.0 89.0	11.3 88.7	11.2 88.8
E(n→σ*)	-	0.7	1.4	2.9
ΔE _{int}	-	6.8	1.1	2.2

^a The difference in the Si-H distance between the monomer and complex. ^b Energies are given in kcal/mol.

(B) Promotion of Improper Behavior. The same two factors as described above control other types of recently reported improper H-bonds involving Si-H,⁸ P-H,⁸ and N-H^{8,9} moieties. We will analyze these complexes in order to illustrate which properties of the H-bond donor favor formation of an improper H-bond. In the final part, we will report the first examples of neutral improper H-bonded complexes with participation of O-H bonds (Table 5).

Si-H...Y Bonds. Let us start with H-bonded complexes of SiF₃H (X) with various acceptors and donors (Y = H₂O, H₂S, and NH₃). In this case, the contribution from hyperconjugation is so small that improper H-bonding is observed in all cases even in the complex with NH₃ which was red-shifted in the case of CHF₃. The nitrogen lone pair in NH₃ is a relatively strong donor which leads to considerable deviation of the Si-H bond for this complex from correlation in Figure 17 but is not sufficiently strong to result in a net red-shift unlike in the case of CF₃H.

Increased likelihood of improper H-bonding in Si-H...Y systems is a consequence of unfavorable polarization of Si-H bonds which, via a combination of two effects, results in formation of complexes that are weaker and less tightly bound compared with their C-H...Y analogues. First, it decreases the electrostatic component of the binding energy (in fact, natural charge on hydrogen atom in HSiF₃ is negative!). Second, it decreases the hyperconjugative component of the binding energy which parallels the decrease in acceptor ability of σ*(Si-H) orbitals compared to that of σ*(C-H) orbitals. Because σ(Si-H) bonds are polarized in an opposite direction than σ(C-H), the σ*(Si-H) orbitals which mirror the polarization of σ(Si-H) orbitals have a larger coefficient on Si and a smaller coefficient on H. Thus, the polarization of σ*(Si-H) orbital is unfavorable for the hyperconjugative n(Y)...σ*(Si-H) interac-

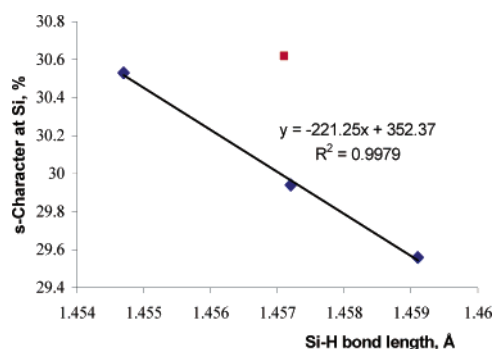

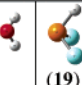
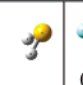


Figure 17. Correlation of Si-H bond lengths with s-character in Si-H bonds of **11–13** at MP2/6-31+G* level (diamonds). Note that although hyperconjugative n(N)→σ*(Si-H) interaction in complex **14** (a square) leads to noticeable deviation from the correlation, it is still not able to provide net Si-H bond lengthening compared to the isolated HSiF₃ molecule.

Table 6. NBO Analysis on the Improper H-bonded Complexes of PF₂H (X) with H₂O, H₂S and NH₃ at the MP2/6-31+G* Level^b

Parameter	PF ₂ H	 (18)	 (19)	 (20)
P-H, Å	1.4202	1.4143	1.4176	1.4149
Δr ^a	-	0.0059	0.0026	0.0053
P-F, Å	1.628	1.635	1.633	1.645
X...Y, Å	-	2.384	2.630	2.716
q _P	1.428	1.392	1.423	1.422
q _H	-0.144	-0.103	-0.130	-0.135
q _F	-0.642	-0.646	-0.647	-0.659
q _{CT}	-	0.003	0.001	0.032
n(σ _{PH})	1.9783	1.9766	1.9771	1.9747
n(σ _{PF})	1.9932	1.9934	1.9930	1.9926
n(σ* _{PH})	0.0255	0.0269	0.0254	0.0263
n(σ* _{PF})	0.0409	0.0405	0.0404	0.0533
n(LP _Y)	-	1.9998	2.0000	2.0000
n(LP _Y) _{X,Y}	-	1.9949	1.9977	1.9632
spn (PH)	sp6.00	sp5.48	sp5.90	sp5.54
% s-character	13.89	15.01	14.10	14.87
spn (PF)	sp7.66	sp7.71	sp7.82	sp8.46
% s-character	11.20	11.13	10.99	10.32
pol (σ _{PH}), P% H%	42.8 57.2	44.9 55.1	43.5 56.5	43.1 56.9
pol (σ _{PF}), P% F%	15.4 84.6	15.3 84.7	15.2 84.8	14.8 85.2
E(n→σ*)	-	3.6	0.3	0.5
ΔE _{int}	-	2.4	2.9	8.1

^a The difference in the P-H distance between the monomer and complex. ^b Energies are given in kcal/mol.

tions. As a result, the range of hyperconjugative donors able to form improper H-bonds is expanded for HSiF₃ compared to CHF₃.

P-H...Y Bonds. Analysis of P-H...Y H-bonds reveals the blue-shifting behavior in all H-bonded complexes listed in Table 6 as well as other properties which are quite similar to those of Si-H...Y complexes. Although the lack of dominant H-bonding interactions in some of these complexes complicates analysis of the general trends, it is obvious that n(Y) → σ*(P-H) hyperconjugation is weak. As a result, the role of rehybridization in controlling the P-H bond length is dominant as illustrated in Figure 18. Interestingly, in this case the oxygen lone pair in complex **18** is a better hyperconjugative donor in n(Y) → σ*(P-H) interactions than its nitrogen counterpart in complex **20** (in contrast to n(Y) → σ*(Si-H) interactions in complexes **12**, **14**). This observation is readily explained by the different

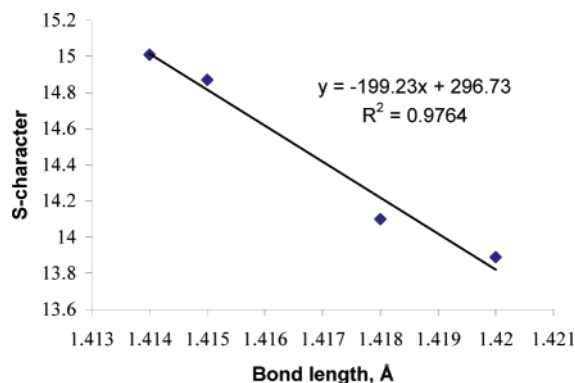
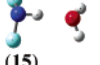
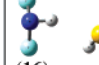
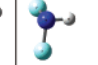


Figure 18. Correlation of P–H bond lengths with s-character in P–H bonds at MP2/6-31+G* level.

Table 7. NBO Analysis on the H-bonding Complexes of NF₂H (X) with Various Acceptors and Donors (Y = H₂O, H₂S and NH₃) Computed at the MP2/6-31+G* Level

Parameter	NF ₂ H	 (15)	 (16)	 (17)
N–H, Å	1.0298	1.0327	1.0323	1.0409
Δr ^a	-	0.0029	0.0025	0.0111
N–F, Å	1.416	1.422	1.419	1.424
H...Y, Å	-	1.914	2.519	1.934
q _N	0.213	0.189	0.199	0.176
q _H	0.381	0.420	0.393	0.408
q _F	-0.297	-0.315	-0.305	-0.320
q _{CT}	-	0.020	0.024	0.038
n(σ _{NH})	1.9889	1.9905	1.9901	1.9911
n(σ _{NF})	1.9944	1.9949	1.9949	1.9951
n(σ* _{NH})	0.0095	0.0270	0.0298	0.0440
n(σ* _{NF})	0.0334	0.0316	0.0320	0.0311
n(LP _N)	-	1.9998	2.0000	1.9997
n(LP _N) _{X,Y}	-	1.9787	1.9765	1.9601
spn (NH)	sp3.00	sp2.44	sp2.62	sp2.26
% s-character	24.93	28.96	27.53	30.58
spn (NF)	sp6.49	sp6.96	sp6.80	sp7.14
% s-character	13.30	12.50	12.75	12.22
pol (σ _{NH}), N%	69.3	72.0	70.7	72.9
H%	30.7	28.0	29.3	27.1
pol (σ _{NF}), N%	34.0	33.1	33.5	32.9
F%	66.0	66.9	66.5	67.1
E(n→σ*)	-	18.7	12.7	28.1
ΔE _{int}	-	8.6	5.0	11.0


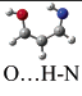
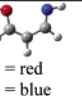
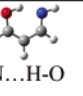
^a The difference in the N–H distance between the monomer and complex.

^b Energies are given in kcal/mol.

geometries of the complexes (Table 5 and Table 6). In PF₂H...NH₃ complex **20**, where the HPN angle is close to 90° and the P–H...N contact can hardly be classified as a hydrogen bond (similarly to the Si–H...O contact in complex **12**). In general, the observed geometries result from a tradeoff between X–H...Y H-bonding and several other attractive interactions (i.e., n(F) → σ*(S–H) in **19**). For many of these systems, there are several complexes with similar binding energies. Because detailed study of all of these complexes would require a separate paper and, to keep the discussion simple, we have considered only a single energy minimum for such systems in this paper.

N–H...Y Bonds. N–H...Y H-bonds are interesting because nitrogen is more electronegative than carbon and σ*(N–H) orbitals are better acceptors than σ*(C–H) orbitals. In accord with this notion, the role of N–H bond lengthening hyperconjugative interactions increases and only classic red-shifted

Table 8. NBO Analysis on the H-bonding for the Syn and Anti Isomers of 3-Imino-propen-1-ol Computed at the MP2/6-31+G*

Parameter	 O = red N = blue	 O...H-N	 O = red N = blue	 N...H-O
X–H, Å	1.0267	1.0254	0.9734	1.0069
Δr ^a	-	-0.0013	0.0000	0.0335
H...Y, Å	-	2.143	-	1.751
q _X	-0.686	-0.686	-0.746	-0.797
q _H	0.364	0.381	0.510	0.567
n(σ _{XH})	1.9797	1.9803	1.9900	1.9869
n(Y _{LP})	1.9851	1.9820	1.9622	1.9164
n(σ* _{XH})	0.0063	0.0125	0.0044	0.0575
spn (XH)	sp3.41	sp3.04	sp3.65	sp2.52
% s-character	22.59	24.69	21.30	28.35
pol (σ _{XH}), X%	68.1	69.3	75.6	80.7
H%	31.9	30.7	24.4	19.3
E(n→σ*)	-	4.0	-	36.6
ΔE _{int}	-	3.1	-	15.8

^a The difference in the X–H distance between the monomer and complex.

H-bonding is observed for the cases illustrated in Table 7 (eventually despite the fact that the changes in s-character of the N–H bonds are larger than those for the C–H bonds).

Nevertheless, in an N–H...Y system where H and Y are spatially close but not oriented optimally for the orbital overlap needed for N–H bond lengthening n(Y) → σ*(N–H) hyperconjugative interaction, improper H-bonding is possible even for N–H bonds. This is illustrated below using a system reported by Guo and co-workers^{9,46} who found that formation of intramolecular N–H...O bond in the *syn*-conformer of 3-imino-propen-1-ol leads to decrease in the N–H bond length (Table 8). Although the authors attributed this observation to steric factors,⁹ the same balance of hyperconjugation and rehybridization readily explains this case. Another example of an improper N–H...Y bond was recently reported by Hobza and co-workers in NF₂H...FH system.⁴⁷

O–H...Y Bonds. A large contrast between N–H...O and O–H...N H-bonding patterns in 3-imino-propen-1-ol illustrates the notion that O–H bonds are less likely to display the blue-shift than N–H bonds even when geometries result in large steric interaction. In fact, N...O distance in the O–H...N H-bonded complex in Table 8 is even shorter than that in the corresponding N–H...O complex (2.636 Å vs 2.940 Å). Classic H-bonding in the O–H...N system is not surprising because σ*(OH) orbitals are much stronger hyperconjugative acceptors than all other X–H bonds discussed in this paper (X = C, Si, P, N). In addition, OH bonds are the most polar and have the lowest polarizability in these series. As the result, improper ROH...Y bonds with participation of alcohols were, to the best of our knowledge, so far not known.⁴⁸

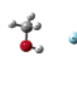
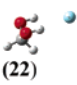
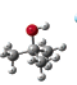
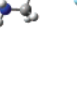
Below we report the first two families of H-bonded O–H...Y complexes which were directly predicted by our model. Blue-shifted O–H complexes are rare because σ*(OH) are among the strongest sigma acceptors. However, when Y is a very weak hyperconjugative donor and the energy of hyperconjugative n(Y) → σ*(O–H) interaction is below the 3–5 kcal/mol threshold,

(46) Note that Schlegel and co-workers also reported a similar example in ref 8.

(47) Hobza, P. *Int. J. Quantum Chem.* **2002**, *90*, 1071.

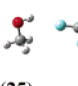
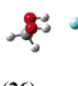
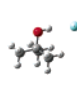
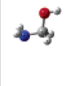
(48) Note that OH stretching frequencies of OH[−] ions can exhibit blue shift upon complexation with metal ions. See Hermansson, K. *J. Chem. Phys.* **1991**, *95*, 3578 and references therein for a thorough discussion.

Table 9. NBO Analysis of Complexes of Alcohols (ROH, where R = Me, CH₂OH, *t*-Bu, NH₂CH₂) with Neon and their Interaction Energies at the MP2/6-31+G* Level

parameter ^a	MeOH	 (21)	 CH ₂ - (OH) ₂ (22)	 <i>t</i> -BuOH (23)	 H ₂ N- CH ₂ OH (24)			
O-H, Å	0.9718	0.9714	0.9732	0.9728	0.9758	0.9751	0.9739	0.9732
Δr ^d	-	-0.0004	0.0000	-0.0004	0.0000	-0.0007	0.0000	-0.0007
H...Ne, Å	-	2.5614	-	2.6396	-	2.5605	-	2.5376
q _O	-0.818	-0.819	-0.816	-0.817	-0.824	-0.825	-0.817	-0.818
q _H	0.494	0.495	0.492	0.493	0.490	0.491	0.493	0.494
q _{CT}	-	0.0006	-	0.0007	-	0.0008	-	0.0007
n(σ _{OH})	1.9928	1.9927	1.9918	1.9918	1.9909	1.9909	1.9906	1.9906
n(σ* _{OF})	0.0048	0.0054	0.0062	0.0066	0.0056	0.0064	0.0038	0.0045
n(Lp _{Ne})	-	2.0000	-	2.0000	-	2.0000	-	2.0000
n(Lp _{Ne}) _{complex}	-	1.9993	-	1.9992	-	1.9992	-	1.9992
spn (OH)	sp3.62	sp3.59	sp3.55	sp3.53	sp3.69	sp3.65	sp3.70	sp3.66
% s-character	21.56	21.73	21.88	22.00	21.26	21.44	21.21	21.41
pol, O%	74.82	74.87	74.78	74.81	74.66	74.72	74.71	74.78
(σ _{OH}) H%	25.18	25.13	25.22	25.19	25.34	25.28	25.29	25.22
E(n→σ*)	-	0.55	-	0.30	-	0.60	-	0.66
ΔE _{int} ^a	-	0.41	-	0.57	-	0.52	-	0.38
ΔE _{int} (ZPE) ^b	-	0.23	-	0.34	-	0.30	-	0.22
ΔE _{int} (BSSE) ^c	-	-0.02	-	-0.06	-	0.02	-	-0.03

^a The interaction energies of the complexes. ^b The energies after zero-point correction. ^c The BSSE-corrected energies. ^d The difference in the O-H distance between the monomer and complex.

Table 10. NBO Analysis on the Complexes of ROH (R = Me, CH₂OH, *t*-Bu, NH₂CH₂) with CF₄ and Their Interaction Energies (kcal/mol) at the MP2/6-31+G* Level

parameter ^a	MeOH	 (25)	 CH ₂ - (OH) ₂ (26)	 <i>t</i> -BuOH (27)	 H ₂ N- CH ₂ OH (28)			
O-H, Å	0.9718	0.9714	0.9732	0.9728	0.9758	0.9747	0.9739	0.9748
Δr ^d	-	-0.0004	0.0000	-0.0004	0.0000	-0.0011	0.0000	0.0009
H...F, Å	-	2.3511	-	2.3892	-	2.3617	-	2.3915
q _O	-0.818	-0.821	-0.816	-0.819	-0.824	-0.827	-0.817	-0.847
q _H	0.494	0.497	0.492	0.495	0.490	0.494	0.493	0.495
q _{CT}	-	0.0006	-	0.0014	-	0.0020	-	0.0008
n(σ _{OH})	1.9928	1.9927	1.9918	1.9918	1.9909	1.9908	1.9906	1.9905
n(σ* _{OF})	0.0048	0.0061	0.0062	0.0075	0.0056	0.0069	0.0038	0.0059
n(Lp _F)	-	1.9879	-	1.9879	-	1.9879	-	1.9879
n(Lp _F) _{complex}	-	1.9872	-	1.9870	-	1.9869	-	1.9873
spn (OH)	sp3.62	sp3.53	sp3.55	sp3.48	sp3.69	sp3.59	sp3.70	sp3.52
% s-character	21.56	22.02	21.88	22.26	21.26	21.73	21.21	22.09
pol, O%	74.82	75.00	74.78	74.96	74.66	74.87	74.71	75.01
(σ _{OH}) H%	25.18	25.00	25.22	25.04	25.34	25.13	25.29	24.99
E(n→σ*)	-	1.27	-	0.87	-	1.36	-	1.09
ΔE _{int} ^a	-	1.42	-	2.84	-	1.68	-	6.44
ΔE _{int} (ZPE) ^b	-	1.23	-	2.45	-	1.49	-	5.82
ΔE _{int} (BSSE) ^c	-	0.19	-	0.78	-	0.31	-	5.24

^a The interaction energies of the complexes. ^b The energies calculated after zero-point correction. ^c The BSSE-corrected energies. ^d The difference in the O-H distance between the monomer and complex.

O-H...Y systems display all characteristic features of improper H-bonding. NBO analyses of two families of such complexes (X = Ne and CF₄) are given in Table 9 and Table 10, respectively. Although the complexes with Ne exhibit directionality characteristic for classic H-bonds and their binding energies before the BSSE correction are very close in their magnitude to the magnitude of n(Y) → σ*(O-H) hyperconjugative interactions, their binding energies are very small especially after the counterpoise correction. Note, however, that the counterpoise correction for BSSE sometimes makes the results less accurate⁴⁹ and absolute energies in Table 9 and Table

10 should be taken with caution. In any case, the complexes with tetrafluoromethane are stronger and should be observable experimentally, especially in those cases when several intermolecular contacts are present.

4. Relation to Other Models of Improper H-Bonding and General Consequences of Hyperconjugation/Rehybridization Model. Although the rehybridization model fits well into the framework of classic structural organic chemistry, it is important to define its relationship to other models developed in the

(49) Xantheas, S. S.; Burnham, C. J.; Harrison, R. J. *J. Chem. Phys.* **2002**, *116*, 1493.

literature. Encouragingly, this model is consistent with both schools of thought concerned with the nature of H-bonding. First, it is consistent with observations of structural reorganization in remote parts of the H-bond donor noticed by Hobza and co-workers⁷ with the only difference that there is no need to invoke the “two-step mechanism” (electron density transfer from a lone pair to “the remote part of the proton donor, causing it to structurally relax” as a first step, followed by shortening of the C–H bond as a second step).⁵⁰ At the same time, our model consistent with the unified picture of proper and improper H-bonding outlined in the Introduction and complements it by providing the mechanism for the improper H-bonding. Because rehybridization is associated with repolarization, our model overlaps nicely with more quantitative repolarization model of vibrational frequency shifts in weak molecular complexes developed by Dykstra and co-workers¹⁶ and with the observations of Dannenberg and co-workers.¹⁷ Differences in behavior of O–H and C–H bonds in external electric field discussed by Qian and Krimm also are consistent with our model.¹⁹ Moreover, our model points out to the regions where the differences disappear and even O–H bonds can participate in the formation of improper H-bonds.

The importance of this simple model increases when one realizes that improper H-bonds are likely to be involved in many phenomena in biological chemistry, molecular recognition and materials science. For example, weak C–H-bonds are increasingly recognized as an important force in molecular recognition,^{51,52} protein structure and function,^{52,53} design of environmentally friendly processes,⁵⁴ crystal engineering⁵⁵ among many other fields. For a long time, the very existence of these weak H-bonds was debated because no “characteristic” red shift in IR stretching frequency was observed (“no red shift—no hydrogen bond”). In contrast with this early notion, the discovery of improper H-bonding proved that many stabilizing contacts do not lead to the red shift and an overhaul of general paradigms in the above fields may be required. The general trends analyzed in this paper should be useful for this purpose. Because changes in hybridization can be easily observed through direct NMR C–H coupling constants, this theoretical model can be experimentally tested by simple NMR studies.

In addition, the interplay of these two competing factors influencing covalent bond length is not limited to H-bonding

but should be applicable to other noncovalent complexes⁵⁶ as well to an understanding of intramolecular stereoelectronic effects on molecular geometry.⁵⁷

Conclusion

Improper H-bonding is not a surprising aberration but rather a logical consequence of one of the most general rules of structural organic chemistry known as Bent’s rule, which predicts an increase in s-character in X–H bonds upon X–H...Y H-bond formation because H becomes more electropositive during this process. The observed structural reorganization of X–H bonds in the process of both “proper” and “improper” H-bonding results from a balance of hyperconjugative bond weakening and rehybridization promoted bond strengthening. These two effects are general for all types of H-bonds and, thus, there is no fundamental difference between classic and improper H-bonding.

Improper H-bonding is likely to be observed only when the X–H bond elongating hyperconjugative $n(Y) \rightarrow \sigma^*(X-H)$ interaction is relatively weak (NBO energy for this interaction is less than 3 kcal/mol). Improper H-bonds have so far been observed more generally for C–H bonds because C–H bonds are weaker σ -acceptors than O–H or N–H bonds. Recent findings of improper behavior of other weak σ -acceptors such as Si–H, P–H indicates the general importance of this phenomenon. Moreover, under circumstances when hyperconjugation in X–H...Y systems is weak, improper H-bonding is possible for N–H and even for O–H bonds.

For improper H-bonding to occur, the molecular structure should allow significant rehybridization of the X–H bond upon formation of the complex. If molecular structure inhibits rehybridization, only the classic red-shift H-bonding will be observed even for X–H bonds with relatively weak hyperconjugative σ -acceptor ability.

Acknowledgment. I.A. is grateful to Florida State University for a First Year Assistant Professor Award, to the Donors of the American Chemical Society Petroleum Research Fund for partial support of this research, and to the 3M company for an Untenured Faculty Award. He also thanks Professor P. Hobza for bringing the problem of improper H-bonding to his attention and to Professor Werner Herz and Robert Fulton for helpful suggestions.

Supporting Information Available: Cartesian coordinates and absolute energies of all stationary point geometries. Complete NBO analysis on the improper H-bonding complexes of CF₃H (X) at the B3LYP/6-311+G** level. Complete NBO analysis of the all points for all points in O...H and Cl...H distance scans in CHF₃/water and CHF₃/water complexes. This material is available free of charge via the Internet at <http://pubs.acs.org>.

JA034656E

- (50) van der Veken, B. J.; Herrebout, W. A.; Szostak, R.; Shchepkin, D. N.; Havlas, Z.; Hobza, P. *J. Am. Chem. Soc.* **2001**, *123*, 12 290.
- (51) Chang, H.-C.; Lee, K. M.; Jaing, J.-C.; Lin, M.-S.; Lin, I. J. B.; Lin, S. H. *J. Chem. Phys. A* **2002**, *117*, 1723. Lindeman, S. V.; Kosynkin, D.; Kochi, J. K. *J. Am. Chem. Soc.* **1998**, *120*, 13 268. Hunter, C. A. *Chem. Soc. Rev.* **1994**, *23*, 101. Hunter, C. A.; Sanders, J. K. M. *J. Am. Chem. Soc.* **1990**, *112*, 5525. Askew, B.; Ballester, P.; Buhr, C.; Jeong, K. S.; Jones, S.; Parris, K.; Williams, K.; Rebek, J. *J. Am. Chem. Soc.* **1989**, *111*, 1082. Zimmerman, S. C.; VanZyl, C. M.; Hamilton, G. S. *J. Am. Chem. Soc.* **1989**, *111*, 1373. Shepodd, T. J.; Petti, M. A.; Dougherty, D. A. *J. Am. Chem. Soc.* **1988**, *110*, 1983. Rebek, J. *Angew. Chem., Int. Ed. Engl.* **1990**, *29*, 245. Diedrich, F. *Angew. Chem., Int. Ed. Engl.* **1988**, *27*, 362.
- (52) Kim, K. S.; Tarakeshwar, P.; Lee, J. Y. *Chem. Rev.* **2000**, *100*, 4145. Brutschy, B. *Chem. Rev.* **2000**, *100*, 3891.
- (53) Krimm, S.; Kuroiwa, K. *Biopolymers* **1968**, *6*, 401. Krimm, S. *Nature* **1966**, *212*, 1482. Scheiner, S.; Kar, T.; Gu, Y. *J. Biol. Chem.* **2001**, *276*, 9832. Burely, S. K.; Petsko, G. A. *Science* **1985**, *229*, 23. Blundell, T.; Singh, J.; Thornton, J.; Burley, S. K.; Petsko, G. A. *Science* **1986**, *234*, 1005. Burely, S. K.; Petsko, G. A. *J. Am. Chem. Soc.* **1986**, *108*, 7995. Brandl, M.; Weiss, M. S.; Jabs, A.; Suhnel, J.; Hilgenfeld, R. *J. Mol. Biol.* **2001**, *307*, 357. Toth, G.; Murphy, R. F.; Lovas, S. *Protein Eng.* **2001**, *14*, 543.
- (54) Blatchford, M. A.; Raveendran, P.; Wallen, S. L. *J. Am. Chem. Soc.* **2002**, *124*, 14 818.
- (55) Desiraju, G. R. *Acc. Chem. Res.* **1996**, *29*, 441.

- (56) Bauschlicher, C. W., Jr. *Int. J. Quantum Chem.* **1997**, *61*, 859. Bagus, P. S.; Nelin, C. J.; Muller, W.; Philpott, M. R.; Seki, H. *Phys. Rev. Lett.* **1987**, *58*, 559. Bertran, J. F.; Ruiz, E. R. *Spectrochim. Acta* **1993**, *49A*, 43.
- (57) For example, the competing role of hyperconjugation and changes in s-character can explain unusual structural effects such as reverse Perlin effects in certain C–H bonds in dithiane. Alabugin I. V. *J. Org. Chem.* **2000**, *65*, 3910–3919.